

# NUMERICAL INVESTIGATIONS ON SYNTHETIC JET IMPINGEMENT COOLING USING MULTIPLE ORIFICE

PROJECT REPORT

submitted by

**VAISHNAV S**

**Reg. No: TKM21MEIR11**

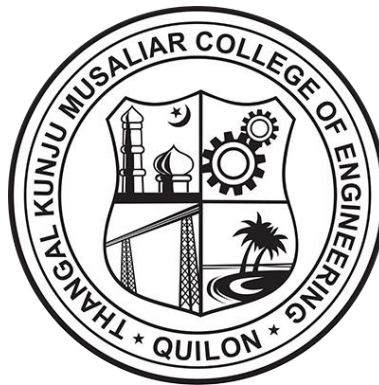
to

the APJ Abdul Kalam Technological University  
in partial fulfilment of the requirements for the award of the Degree of  
*Master of Technology*

*in*

*Mechanical Engineering*

*Specialization: Industrial Refrigeration and Cryogenic Engineering*



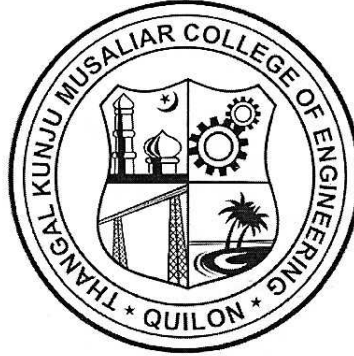
**Department of Mechanical Engineering**

**THANGAL KUNJU MUSALIAR COLLEGE OF ENGINEERING, KOLLAM**

**MAY 2023**

**DEPARTMENT OF MECHANICAL ENGINEERING**

**TKM COLLEGE OF ENGINEERING, KOLLAM**



**CERTIFICATE**

This is to certify that this report entitled "NUMERICAL INVESTIGATIONS ON SYNTHETIC JET IMPINGEMENT COOLING USING MULTIPLE ORIFICE" is the report of project presented by VAISHNAV S, Reg. No: TKM21MEIR11 during 2022 -2023 to the APJ Abdul Kalam Technological University in partial fulfilment of the requirements for the award of the Degree of Master of Technology in Industrial Refrigeration and Cryogenic Engineering is a bonafide record of the project work carried out by him under my guidance and supervision. This report in any form has not been submitted to any other University or Institute for any purpose.

Internal Supervisor:

**Dr. Leena R**

Assistant professor

Department of Mechanical Engineering

TKM College of Engineering , Kollam-5

PG Coordinator:

**Dr. Shafi K A**

Professor

Department of Mechanical Engineering

TKM College of Engineering , Kollam-5

Head of the Department:

**Dr. Dileep P N**

Professor

Department of Mechanical Engineering

TKM College of Engineering, Kollam-5

## DECLARATION

I, **Vaishnav S** hereby declare that, this project report entitled “Numerical Investigations of Synthetic Jet Impingement Cooling Using Multiple Orifice” is the bonafide work of mine carried out under the supervision of **Dr. Leena R**, Assistant Professor, Department of Mechanical Engineering, TKM College of Engineering, Kollam. I declare that, to the best of my knowledge, the work reported herein does not form part of any other project report or dissertation on the basis of which a degree or award was conferred on an earlier occasion to any other candidate. The content of this report is not being presented by any other student to this or any other University for the award of a degree.

**Vaishnav S** 

Register No: **TKM21MEIR11** of year **2021-23**

May 2023

Internal Supervisor:



**Dr. Leena R**

Assistant Professor

Department of Mechanical Engineering

TKM College of Engineering , Kollam-5

Head of the Department:



**Dr. Dileep P N**

Professor

Department of Mechanical Engineering

TKM College of Engineering , Kollam-5

## ACKNOWLEDGEMENT

Any attempt at any level cannot be satisfactorily completed without the support and guidance of learned people. I take this opportunity to express my deep sense of gratitude and sincere thanks to all who helped us to complete the seminar successfully.

Firstly, I would like to express my heartfelt thanks to **Dr. Leena R.**, Assistant professor, Department of Mechanical Engineering, TKM College of Engineering for being instrumental in the completion of my project with his guidance. I express my deep sense of gratitude to thank **Dr. Dileep P.N.**, Professor and Head of Department, Department of Mechanical Engineering, TKM College of Engineering for the support to complete this project. I thank **Dr. Shafi K.A.**, PG coordinator, Department of Mechanical Engineering, TKM College of Engineering for giving their constant support for doing this project. I thank **Dr. Arun Jacob**, Assistant professor, Department of Mechanical Engineering, MES Institute of Technology and Management for his constant support regarding the proceedings of the project.

Finally, I thank our parents and friends near and dear ones who directly and indirectly contributed to the successful completion of my project.

May 2023

VAISHNAV S

## ABSTRACT

A synthetic jet generally consists of a cavity with a driver attached on one side and an orifice on the opposite side. When the driver moves back and forth, the jet will generate an unsteady flow through the orifice and the flow will move downstream to a surface forming an impinging flow. When the jet is in the ejection cycle, the diaphragm will expel flow out from the orifice and form a vortex near the orifice. If the propulsion is large enough, the vortex will move downstream before the jet orifice flow reverses and starts to suck in flow. The computational process is carried out using the commercial software ANSYS Fluent. In this study, the heat transfer characteristics of synthetic jet impingement cooling with multiple orifice (2,4 and 16 orifices) are analysed with different operating frequencies ( $f=1\text{Hz}$  to  $f=5\text{Hz}$  and  $f=100\text{Hz}$  to  $f=500\text{Hz}$ ) with different Reynolds number ( $Re=5000, 10000$  and  $20000$ ) well as Strouhal number ( $St=0.006$  to  $St=0.030$ ). The results demonstrate that high frequency synthetic jets show better heat removal capacity than lower frequency at the same Reynolds number. Also, the variation of area-averaged Nusselt number depends on Strouhal number or dimensionless stroke length.

**Keywords:** Synthetic jet impingement, Reynolds number, Frequency, Average-Nusselt number, Multiple orifice, Strouhal number.

# LIST OF CONTENTS

<b>Contents</b>	<b>Page No.</b>
<b>ACKNOWLEDGEMENT</b>	i
<b>ABSTRACT</b>	ii
<b>LIST OF FIGURES</b>	vi
<b>LIST OF TABLES</b>	vii
<b>NOTATIONS</b>	viii
<b>Chapter 1: INTRODUCTION</b>	<b>1</b>
1.1 Background	2
1.2 Thermal management solutions	3
1.3 Objectives	5
1.4 Methodology	5
<b>Chapter 2: LITERATURE REVIEW</b>	<b>7</b>
<b>Chapter 3: PRINCIPLE OF SYNTHETIC JET IMPINGEMENT</b>	<b>10</b>
<b>Chapter 4: CFD SIMULATION</b>	<b>13</b>
4.1 Introduction to CFD	13
4.2 CFD Applications	13
4.3 Numerical methods used in CFD	13
4.3.1 Finite difference method	14
4.3.2 Finite element method	14
4.3.3 Finite volume method	14
4.4 Advantages of CFD	15

4.5 Working of a CFD code	15
4.5.1 Pre-processor	15
4.5.2 Solver	16
4.5.3 Post-processor	16
4.6 CFD Calculation	17
<b>Chapter 5: NUMERICAL STUDY ON HEAT TRANSFER</b>	19
5.1 Geometric model	19
5.2 Grid generation	21
5.3 Fluent analysis	24
5.3.1 Boundary conditions	25
5.3.2 Input parameters	26
5.3.3 Solution technique	27
5.3.2 Convergence criteria	27
<b>Chapter 6: EQUATIONS AND NUMERICAL CALCULATIONS</b>	28
<b>Chapter 7: RESULTS AND DISCUSSION</b>	30
7.1 Mesh Independent Study	30
7.2 Validation of Numerical Results	31
7.3 Effect of high and low frequencies on average Nusselt number	32
7.3.1 Variation of average Nusselt number with High Frequencies at Re=20000	32
7.3.2 Variation of average Nusselt number with High Frequencies at Re=15000	32
7.3.2 Variation of average Nusselt number with High Frequencies at Re=10000	34

7.3.4 Conclusion from the High frequency analysis	34
7.3.5 Variation of average Nusselt number with Low Frequencies	35
7.3.6 Conclusion from the High frequency analysis	37
7.4 Dependence of local Nusselt number in radial direction	37
7.5 Effect of Reynolds number on heat transfer	38
7.6 Dependence of heat transfer on number of orifices	39
7.7 Effect of Strouhal number on heat transfer	40
7.8 Effect of static temperature distribution	43
7.9 Effect of static static velocity distribution	44
<b>Chapter 8: CONCLUSION AND SCOPE OF FUTURE WORK</b>	47
8.1 Conclusion	47
8.2 Scope of Future Work	48
<b>REFERENCES</b>	49

## LIST OF FIGURES

<b>Figure number</b>	<b>Figure title</b>	<b>Page No.</b>
Fig.1.1	Methods of removing heat from the hot surface	4
Fig.1.2	Methodology flow chart	6
Fig.1.3	Schematic diagram of synthetic jet	11
Fig.1.4	Parameters influencing synthetic jet flow field	12
Fig.5.1	Geometric model and orifice plates	21
Fig.5.2	Mesh domain	22
Fig.7.1	Mesh independent study	30
Fig.7.2	Validation of present study	31
Fig.7.3	Variation of $Nu_{avg}$ with high and low frequencies	36
Fig.7.4	Variation of $Nu_{avg}$ in radial direction of the plate	37
Fig.7.5	Variation of average Nusselt number with Reynolds number	38
Fig.7.6	Variation of average Nusselt number with Strouhal Number	42
Fig.7.7	Variation Temperature distribution on target plate surface	43
Fig.7.8	Pathlines of air jet impingement	43
Fig.7.9	Velocity distribution in 2 orifices	44
Fig.7.10	Velocity vector	45
Fig.7.11	Variation of velocity in radial direction	45

## LIST OF TABLES

<b>No.</b>	<b>Title</b>	<b>Page No.</b>
Table.5.1	Various plates with number of orifices	21
Table.5.2	The effect of mesh size on the obtained results	23
Table.5.3	Input parameters	26
Table.7.1	Validation values of Nusselt number	32
Table.7.2	Range of studied parameters	38

## NOTATIONS

A	Area of heat transfer	$m^2$
B	Base height	m
D	Orifice diameter	m
f	Frequency of oscillation	Hz
h	Average heat transfer coefficient	$W/ m^2K$
k	Thermal conductivity,	$W/ m.K$
L	Length of target wall	M
$L_0$	Stroke length	m
$Nu_{avg}$	Average Nusselt number	
$Nu_A$	Area averaged Nusselt number	
Q	Rate of heat transfer	$W/m^2$
q	Heat flux at target wall	$W/m^2$
Re	Reynolds number	
St	Strouhal number	
t	Time	s
$T_a$	Ambient temperature	K
$T_1$	Wall temperature	K
$U_0$	Mean velocity	m/s
$u(t)$	Instantaneous velocity	m/s

### Greek symbols

$\alpha$	Thermal diffusivity	$m^2/s$
$\mu$	Dynamic viscosity	Pa.s
$\rho$	Density of fluid	$kg/m^3$
$\omega$	Specific dissipation rate	

# CHAPTER 1: INTRODUCTION

Recent developments in micro-technology have led to the miniaturization of electronic devices, while advancements in semiconductor technology have significantly increased their power density. Consequently, ensuring efficient cooling is crucial in the competitive electronic engineering industry, as overheating can cause a decline in device performance. Traditional air cooling systems, such as air-driven fans and heat sink assemblies, struggle to dissipate the high heat fluxes generated by modern electronics. To address this issue, various cooling methods have been developed, including liquid cooling, micro-channel cooling, and active cooling, each with its own strengths and limitations in different applications. Active cooling, which involves stirring the cooling flow to enhance heat transfer, is a promising technology, with piezoelectric fans and synthetic jets being two commonly used active devices that effectively generate turbulence and enhance heat transfer.

Synthetic jet impingement cooling is a promising technology that is being increasingly explored in the field of electronic cooling. As electronic devices become smaller and more powerful, the challenge of dissipating the generated heat becomes increasingly important. Traditional cooling methods such as air-driven fans and heat sink assemblies may not be sufficient to meet the cooling demands of modern electronics, leading to reduced performance and reliability. Synthetic jet impingement cooling, however, offers a more efficient and effective way of cooling electronic devices. By generating small, periodic vortex rings, synthetic jets can stir the cooling flow and enhance heat transfer, resulting in higher cooling performance with lower noise levels and energy consumption. This technology has the potential to revolutionize electronic cooling and pave the way for the development of more advanced and sustainable cooling techniques. In this article, we will explore the principles of synthetic jet impingement cooling, its advantages and limitations, and its applications in various industries.

Enhancing heat transfer is a critical area of engineering research, with the development of highly effective cooling technologies being essential to meet the expanding energy consumption demands and mitigate environmental degradation. Thus, creating new and improved cooling techniques for various thermal equipment is crucial for a sustainable future.

Jet impingement cooling is considered one of the most promising heat transfer augmentation strategies, owing to its ability to achieve rapid heat transfer rates with minimal pressure loss. Impinging jets are utilized in a range of engineering and industrial applications, including drying papers and food products, shaping and tempering glass, annealing plastic and metal sheets, de-icing aircraft wings, and cooling heated parts in gas turbines and miniaturized electronic devices.

## **1.1 BACKGROUND**

Thermal management of electronic devices has become a progressively serious issue for thermal engineers due to miniaturization of electronic components and fast development of integrated circuits that cause the electronics to dissipate higher and higher power. According to Moore's law, the number of transistors on an integrated circuit doubles every 18 months and the transistor density is expected to be more than  $10^{11}$  per die by 2020. The anticipated power density will grow exponentially, as silicon microfabrication technology develops. It is estimated that the power dissipation will increase 13 times as the scales decrease from 90 nm to 15 nm. The heat power has to be carried away by cooling devices to maintain the electronics at a temperature that allows the electronics to work properly.

Traditional steady air cooling systems such as air driven fan and heat sink assemblies have difficulty in dissipating the increasing heat fluxes of modern electronics. The widely-used methods for cooling high heat flux electronics include liquid cooling, micro-channel cooling, and active cooling with their own specific advantages and disadvantages as applied in various fields. The use of electronic equipment has virtually become a necessity in the current environment with numerous new technologies. Due to the significant role this electronic equipment plays in numerous technologically important fields, it has a high component density in a small volume. As a result, during the past few decades, the rate of heat dissipation from electronic components has been steadily rising. Additionally, optimization increased component power, and electronic component heat dissipation has significantly increased. Forcing convection flow was primarily employed by a variety of scientists and researchers to remove heat from component surfaces.

## 1.2 THERMAL MANAGEMENT SOLUTIONS

Thermal management refers to the methods and technologies utilized by engineers and designers to regulate temperatures within a system. These techniques are grounded on the principles of heat transfer and thermodynamics. By implementing thermal management, engineers have the ability to either increase or decrease temperatures and alter the distribution of temperature within a given system. The range of thermal management methods can encompass all modes of heat transfer, including conduction, convection, and radiation, which facilitate the movement of heat from one area to another. This concept has far-reaching implications and finds application in a multitude of industries, from construction to electronic devices to human biology, where the regulation of temperature is crucial for optimal performance.

Different devices have varying temperature thresholds they can withstand, so maintaining optimized temperatures for the specified system is crucial. All circuits and devices generate some excess heat during use, and extremely high temperatures can compromise the operation of any electronic. Most people have experienced the lag that occurs when a computer or smartphone gets too hot. If these problems extend to life-supporting machines, aircraft or electronic components in vehicles or military equipment, the downtime caused by overheating can be dire. To ensure the safety of these circuits and devices, they require thermal management systems.

Designers can use different working fluids and heat transfer technology to move heat away from the device in use. Common strategies for regulating temperature in electronic devices include heating, cooling, heat removal, cycling and temperature homogenization. Engineers can address system temperatures above the ambient temperature with different options for cooling or customized heat transfer technology. Extremely low temperatures can be just as harmful and may require a heating strategy instead. Cycling provides both heating and cooling for the system, with defined temperatures used throughout its run time. Alternatively, the system may need a uniform temperature over a specified length, or area. Temperature homogenization strategies

help mitigate the risk of unwanted fluctuations. All devices have a minimum and maximum operating temperature. Outside of these thresholds, their regular operation becomes potentially compromised.

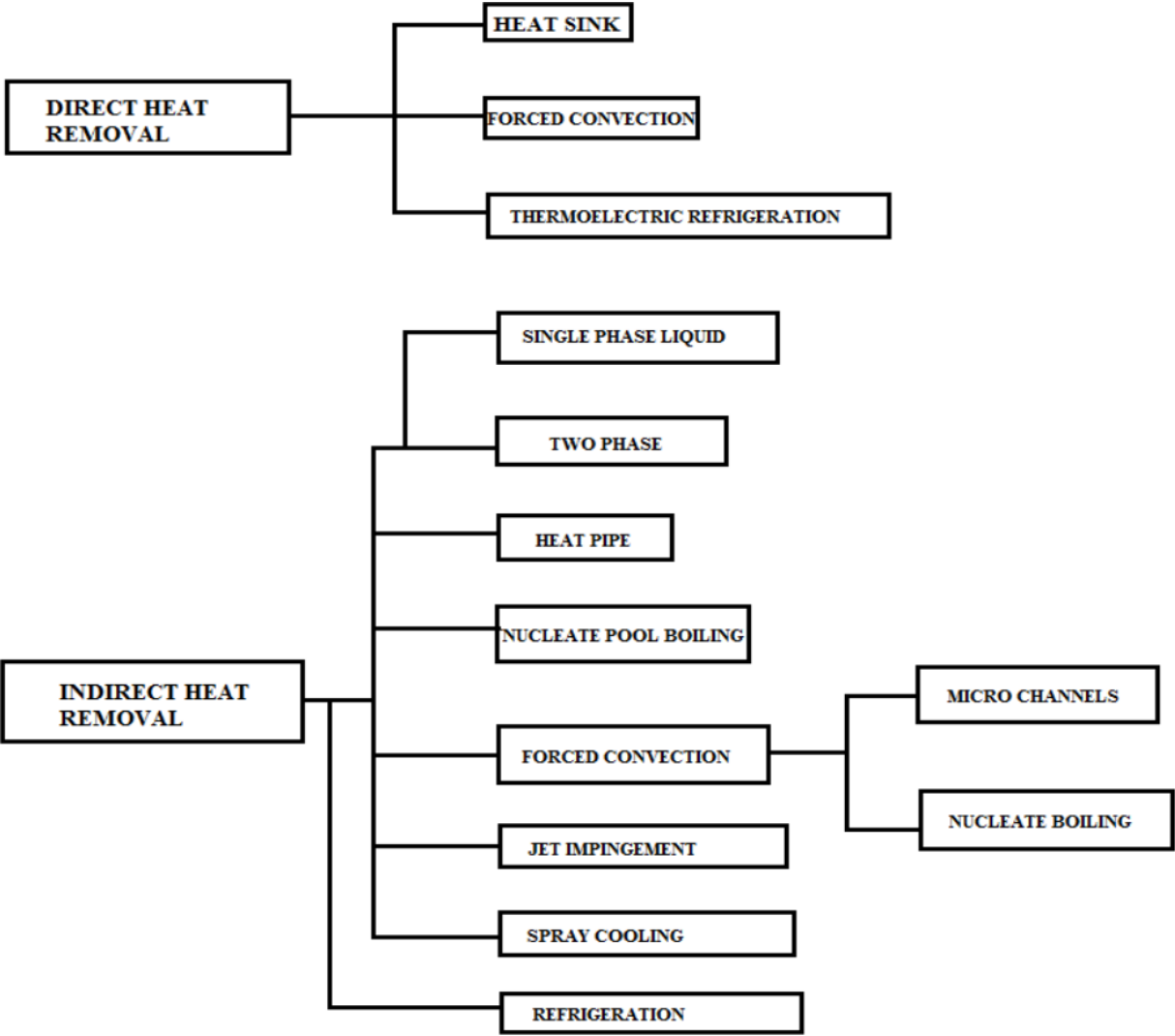


Fig. 1.1. Methods of removing heat from the hot surface.

Electronics that run closer to their upper limit have a shorter service life before they degrade, making operations unsafe and inefficient. Without proper thermal management, these devices may also become too hot to touch and pose risks for the product’s user experience. The resulting downtime and potential hazards caused by overheating systems are unacceptable for medical, defense, aerospace and automotive

applications. When devices made for other applications feature these same problems, it can harm product sales and company reputations. That's why many industries have made thermal management a requirement.

### **1.3 OBJECTIVES**

The main objective is the numerical study (using ANSYS Fluent) on the heat transfer and flow characteristics of synthetic jet impingement cooling using multiple orifice(2,4 and 16 orifices).

The specific objectives are:

1. To validate the numerical model with the experimental values of literature.
2. To study the effect of frequency on the heat transfer characteristics of synthetic jet.
3. To study the effect of Strouhal number and Reynolds number on the heat transfer characteristics of synthetic jet.

### **1.4 METHODOLOGY**

Objective 1: Validate the numerical model with experimental and numerical data from Ping Li et al.(2020).

- Validating the parameters which affect the heat transfer on the hot plate surface.
- Optimizing the parameters such as frequency, Nusselt number and number of orifices.

Objective 2: To study the effect of frequency on the heat transfer characteristics of synthetic jet.

- Selection of frequency range from 1Hz to 5Hz and 100Hz to 500Hz.
- Setting up boundary conditions.
- Numerical simulation with high and low frequencies are carried out by varying the number of orifices.

Objective 3: To study the effect of Strouhal number and Reynolds number on the heat transfer characteristics of synthetic jet.

- Selection of Reynolds number range (10000 to 20000) and Strouhal number range(0.06 to 0.30).
- Setting up boundary conditions.
- Numerical simulation by varying Reynolds number and Strouhal number are carried out with high and low frequency.

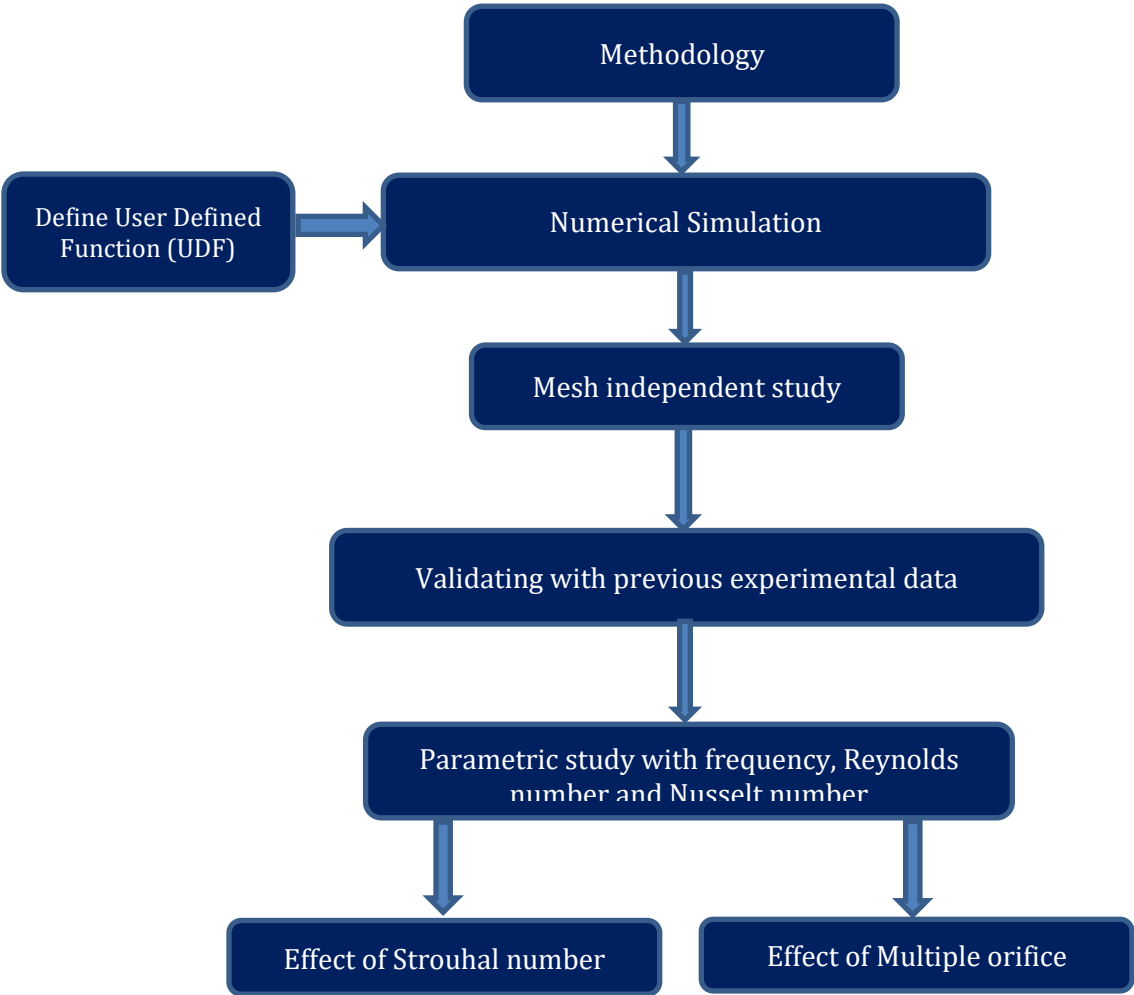


Fig.1.2. Methodology flow chart

## CHAPTER 2 : LITERATURE REVIEW

The characteristic of the local Nusselt number is compared to the work of Cadec [3] and Gardon and Akfirat et al. [13] in order to further validate. Good agreements have been seen overall. For the grid independence study, the grid sizes of 351×171, 381×191, and 401×201 are taken into consideration. The grid independence research, shown in Figure (4), plots non-dimensional variation of wall shear stress for grid sizes 351×171, 381×191, and 401×201. Nonetheless, to be on the safe side, a grid size of 381×191 is chosen for the current computation despite the fact that the change of non-dimensional wall shear stress with three grid levels is relatively modest.

The study by Carlo Salvatore Greco et al. [2] examined the effects of Strouhal numbers (0.011, 0.022, and 0.044) and orifice to plate distances (2, 4, and 6 orifice diameters) on the flow field of an impinging zero-net-mass-flux jet at a Reynolds number of 35000. They discovered that the Strouhal number primarily influences the ZNMF jet structure, controlling how the vortex ring and the following jet impact the flow field. At high Strouhal numbers, the vortex ring causes a faster flow rate and entrainment, resulting in a smaller extension of the potential core, greater centerline turbulent kinetic energy, and a closer starting point for high turbulence level. In contrast, low Strouhal numbers cause the tail jet to be the most significant component of the flow field, leading to a completely different behavior.

A synthetic jet ejector heat sink was created by Mahalingam et al. [14-16] and its thermal performance was evaluated. By including the synthetic jet, the heat sink's thermal resistance can be decreased from 3.15 °C/W to 0.76 °C/W. It was discovered that the heat sink could dissipate 59.2 W of heater power with a temperature difference of under 70°C. In comparison to steady flow in the channel, the heat sink with a synthetic jet was shown to dissipate around 40% more heat.

The heat transfer properties of jet impingement cooling on a copper disc with a diameter of 12.7 mm and a thickness of 6 mm were investigated by Pavlova et al. [10] using a synthetic jet generated by a piezo disc with a diameter of 30.2 mm. The study found that lower frequency jets (420 Hz) were more effective at longer axial distances, while higher frequency jets (1200 Hz) were more effective at shorter distances between the orifice plate and the copper disc. The

researchers also compared the effectiveness of synthetic jets to that of continuous jets at the same Reynolds number and discovered that synthetic jets were three times more efficient in cooling. This intriguing phenomenon was attributed to the buildup of vortex, as observed using Particle Image Velocimetry.

Chaudhari et al.[5] and colleagues investigated the effectiveness of synthetic jet impingement in cross-flow heat transfer by adding fans to the duct. They found that the performance of heat transfer was not significantly impacted by the width of the duct. They achieved the highest heat transfer coefficient ( $134 \text{ W/m}^2\text{K}$ ) using a combination of cross flow and synthetic jet, which was greater than that of cross flow alone but lower than that of synthetic jet impingement alone.

Chaudhari et al.[6] conducted a study to investigate the effect of different orifice configurations on enhancing synthetic jet impingement for heat transfer. They used a larger circular orifice at the center surrounded by several smaller circular orifices to measure the heat transfer coefficients of the satellite orifices. By using a 5mm round hole at the center and eight 3mm round orifices around it, the highest heat transfer coefficient ( $159 \text{ W/m}^2\text{k}$ ) was achieved. This value was 30% higher than that of a single round orifice at the center. It was observed that the heat transfer coefficient for the satellite orifices had two peaks with increasing axial distances, as compared to a single orifice.

Jain et al.[7] the impact of changes in orifice and cavity dimensions on the flow-field of synthetic jets, under similar frequency and amplitude operating conditions. They found that altering the orifice size had a greater influence on the flow-field than modifying the cavity's depth and shape, as long as the amplitude or  $L$  was kept constant. The researchers identified the radius of the orifice and cavity, as well as the thickness of the orifice plate, as the most critical factors affecting the flow-field. In contrast, their experimental work focused on three holes with identical capacity but varying shapes.

Oronzio Manca et al.[9] studied on confined impinging slot jet working with a mixture of water and  $\text{Al}_2\text{O}_3$  nanoparticles. In order to study the behaviour of the system in terms of average and local Nusselt numbers, convective heat transfer coefficient and necessary pumping

power profiles, temperature fields, and stream function contours, various geometric ratios, particle volume concentrations, and Reynolds numbers have been taken into consideration. The dimensionless stream function contours demonstrate how the confining effects, as shown by the H/W ratio, Reynolds number, and particle concentrations, affect the size and intensity of the vortex forms. The local Nusselt number profiles exhibit maximum values at the stagnation point and minimum values near the heated plate's edge. The average Nusselt number rises with increasing particle concentrations and Reynolds numbers. In addition, the highest values are seen for  $H/W = 10$ , and a maximum increase of 18% is found at a concentration of 6%.

Laxmikant Mangate et al.[4] conducted an experimental study to investigate the impact of different orifice shapes on the heat transfer of synthetic air jet impingement, with varying Stokes number and pitch ratio. Their findings indicated that multiple-orifice designs with one and two satellite orifices had a 75% greater heat dissipation compared to a single orifice, only for lower pitch ratio values, showing two local peaks in  $Nu_{avg}$ . The absence of a center orifice resulted in lower heat transmission, and for greater pitch ratios, the maximum value of  $Nu_{avg}$  decreased and shifted closer to the heated surface.

Ping Li et al.[11] numerically investigated Heat transfer and flow structure of  $Al_2O_3$ - $H_2O$  nanofluids periodic pulsating slot-jet impingement with rectangular wave(R-Wave) and triangular wave(T-Wave). T-wave is better than R-wave at enhancing heat transfer through volume fraction and Re for zero-net-mass flow pulsating jets, especially at higher frequencies. Volume fraction and Re both rise with an increase in average Nusselt number, and they also demonstrate a positive reciprocal promotion relationship that improves heat transmission. The frequency-induced trend reveals a nonlinear trend in which the effect of f on the enhancement of heat transfer is weaker at higher frequency. The increment rate of average Nusselt number is lowered up to  $f=20$ Hz. It will be more steady and effective at  $f=20$  Hz than  $f=50$  Hz at higher Re.

Zhuo Liu and colleagues [17] quantitatively investigated the cooling capabilities of synthetic jets and analyzed the impact of nozzle to surface distance on cooling performance. Their findings revealed that as the distance between the nozzle and the surface increases, the cooling ability of synthetic jets initially increases but then decreases.

Ping Li et al.[12] numerical analysis to investigate how the heat transfer behavior of a triangular synthetic jet flow is influenced by Strouhal number, frequency ranging from 10-75Hz, and Reynolds number ranging from 10000 to 20000. Their study revealed that, for a frequency range of 10 to 35 Hz, the moment at which the highest area averaged Nusselt number occurs increasingly lags at identical Reynolds numbers. Moreover, the largest Nusselt number range was found to be within a Strouhal number range of 0.24 to 0.48 for each Reynolds number, although the fluctuation pattern of the area-averaged Nusselt number with normalized time differed from that of Reynolds number when frequency was kept constant. The study concluded that variations in the flow structure, which affect the features of wall jets, vortex behaviour, and the high-speed zone above the target wall, are responsible for the individual effects of Reynolds number and frequency on heat transmission due to the strong coherence between heat and mass transfer.

The study conducted by Museong Kim et al.[8] analyzed how two synthetic jets generated from a dual orifice device interact with each other. The results showed that decreasing the distance between the orifices and reducing the length of the stroke caused the jets to merge and combine more quickly. This was due to the strengthening of the interaction between the two jets, resulting in faster decay of centerline velocity and an increase in symmetry line velocity. On the other hand, increasing the stroke length reduced entrainment and jet interaction due to the influence of the leading vortex ring being diminished and the trailing jet's influence being increased. With increasing stroke length, the merging region grew linearly, and the positions of the merging point and combined point shifted downstream as the distance between the orifices increased.

Arun Jacob et al.[1] investigated examined the effects of the distance between the orifice and the heated plate, as well as the frequency of synthetic air jets, on heat transfer characteristics using both experimental and numerical approaches. They discovered a direct relationship between heat transmission and the frequency of the jet. Furthermore, the optimal  $Z/D$  value was dependent on the jet's frequency, with low  $Z/D$  ratios leading to air entrainment and recirculation, which affected heat transfer efficiency. However, at high  $Z/D$  ratios and frequencies, these effects were mitigated, and uniform heat transfer occurred. The team also noted that the orifice size strongly influenced heat transfer, and synthetic jets exhibited lower heat transfer at very low  $Z/D$  values due to air recirculation.

## CHAPTER 3 : PRINCIPLE OF SYNTHETIC JET IMPINGEMENT

Synthetic jet (SJ) impingement is another innovative method for active cooling. In a simple structure and with a low power requirement, the synthetic jet can produce unsteady, turbulent impinging flow. A synthetic jet is a zero-net mass-flux device widely used in boundary-layer separation control, jet vectoring, mixing enhancement in combustion, and turbulence generation. A synthetic jet generally consists of a cavity with a driver attached on one side and an orifice on the opposite side. When the driver moves back and forth, the jet will generate an unsteady flow through the orifice and the flow will move downstream to a surface forming an impinging flow. When the jet is in the ejection cycle, the diaphragm will expel flow out from the orifice and form a vortex near the orifice. If the propulsion is large enough, the vortex will move downstream before the jet orifice flow reverses and starts to suck in flow. Utturkar et al. proposed a criterion for the formation of the vortices. These vortices are found to enhance mixing and turbulence, and thus, to augment heat transfer performance. Numerous experimental and numerical studies have been conducted in the application of synthetic jets for cooling.

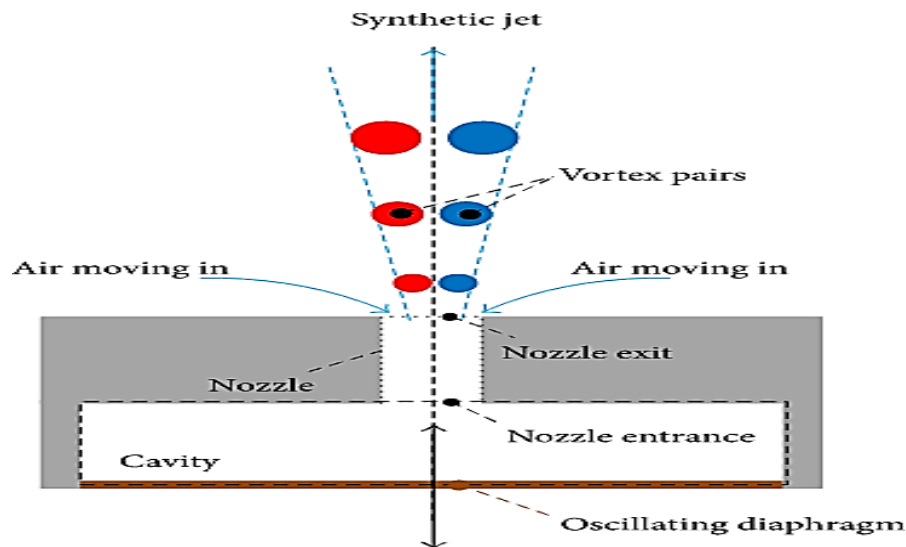


Fig. 1.3. Schematic diagram of synthetic jet.

In recent years, there has been a growing body of literature on Synthetic Jets (SJs) that highlights their potential applications in various industries. These include serving as active flow controlling devices, heat and mass transfer devices, underwater jet propulsion systems, and turbulence mixing enhancers.

Previous research has identified three key parameters that govern the flow-field and performance of SJs: actuation parameters, geometrical parameters, and fluid parameters. These parameters can further be used to derive several dimensionless parameters, including the Reynolds number, Strouhal number, Stokes number, dimensionless stroke-length, and Womersley number. However, researchers have found that only two of these non-dimensional parameters -  $Re$  and  $St$  - are necessary, as they can be correlated using the Buckingham pi-theorem to represent the same characteristic aspects of the SJ flow-field.

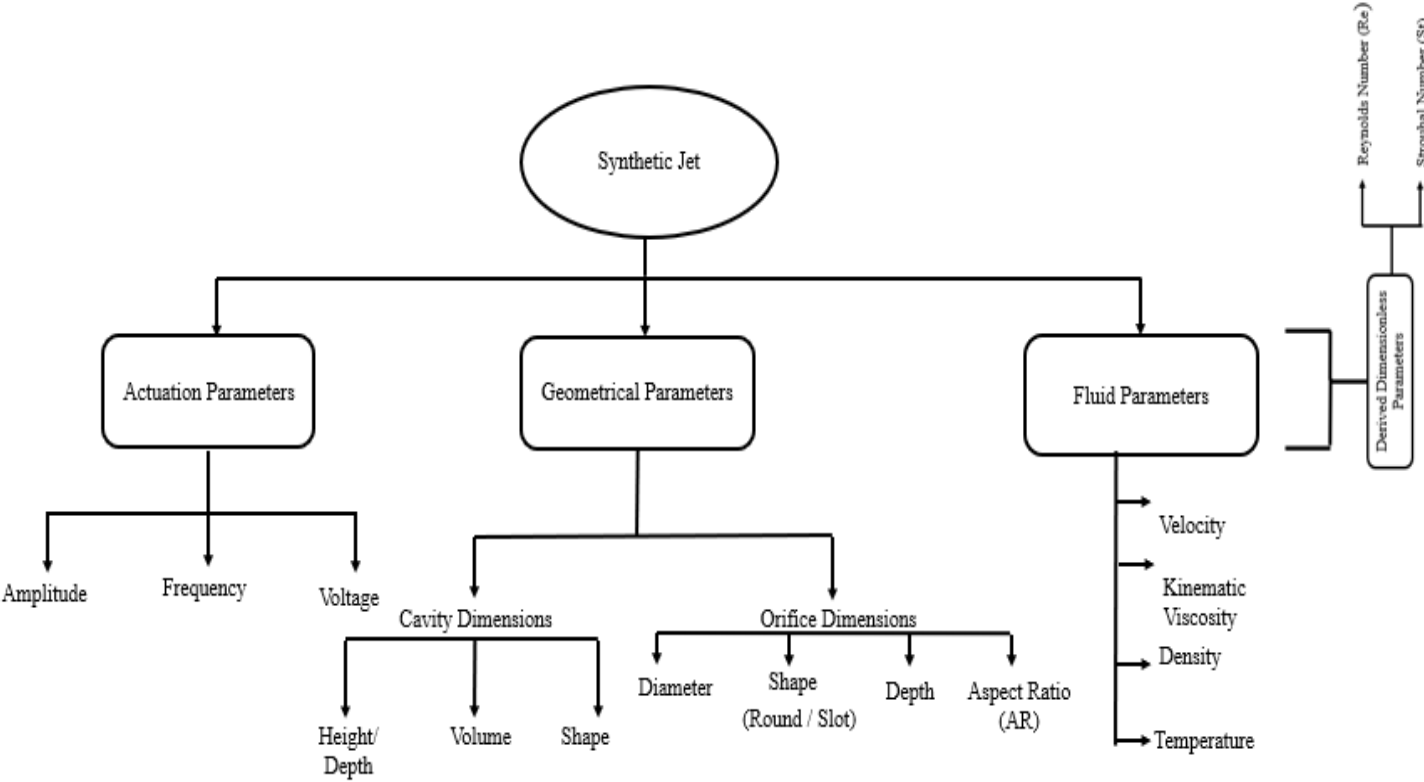


Fig. 1.4. Parameters influencing SJ flow field.

## **CHAPTER 4: CFD SIMULATION**

### **4.1 INTRODUCTION TO CFD**

Computational Fluid Dynamics (CFD) is one of the branches of fluid mechanics that uses numerical methods and algorithms to solve and analyze problems that involve fluid flows. Computers are used to perform the millions of calculations required to simulate the interaction of fluids and gases with the complex surfaces used in engineering. CFD predicts what will happen, quantitatively, when fluid flow, often with the complications of,

- Simultaneous flow of heat.
- Mass transfer.
- Phase change.
- Chemical reaction.
- Mechanical movement.
- Stress and displacement of immersed solids.

### **4.2 CFD APPLICATIONS**

- Aerodynamics of aircrafts and vehicles; lift and drag.
- Hydrodynamics of ships.
- Power plants; combustion in IC engines and gas turbines.
- Turbo machinery; flow inside rotating passages.
- Metrology; weather predictions.
- External and internal environment of buildings; wind loading.

### **4.3 NUMERICAL METHODS USED IN CFD**

The methods used in CFD are;

- Finite Difference Method (FDM).
- Finite Element Method (FEM).
- Finite Volume Method (FVM).

### **4.3.1 Finite Difference Method (FDM)**

The simplest numerical technique to apply for the solution of the heat/diffusion equation is the finite difference method. The basic idea behind the method is to replace the various derivatives appearing in the mathematical formulation of the problem with suitable approximations on finite difference mesh of nodes. The simplest derivation of finite difference formulae makes use of the Taylor series. The final set of linear algebraic equations is solved by any numerical techniques.

### **4.3.2 Finite Element Method (FEM)**

The finite element method subdivides the calculation domain into elements, such as triangular rectangles, tetrahedral or rectangular parallelepipeds elements. These elements are considered interconnected at specified joints called nodes. Here the variation of field variable inside a finite element can be approximated by a simple function. These approximating functions are defined in terms of the values of the field variables at the nodes. When field equations are written for the whole continuum the new unknowns are at the nodal points. By solving the field equations, which are generally in the form of matrix equations, the node values of the field's variables will be known. Once these are known, approximating functions define the field variable through the assemblage of elements.

### **4.3.3 Finite Volume Method (FVM)**

This is the classical or standard approach used most often in commercial software and research codes. An alternative discretization method is based on the idea of regarding the computation domain as subdivided into a collection of finite volumes. In this view, each finite volume is represented by a line in 1D, an area in 2D, and a volume in 3D. Nodes, located inside each finite volume, become the locus of computational values. In rectangular Cartesian coordinates in 2D the simplest finite volumes are rectangles. For each node, the rectangle faces are formed by drawing perpendiculars through the midpoints between contiguous nodes. Discretization equations are obtained by integrating the original partial differential equation throughout each finite volume. This method is easily extended to nonlinear problems. The solutions of the algebraic equations are obtained by iterative methods.

One advantage of this method over FDM is that it does not require a structured mesh - although a structured mesh can be used. The FVM can solve problems on irregular 18 geometries. Furthermore, one advantage of this method over FEM is that it can conserve the variables on a coarse mesh easily. This is an important characteristic of the fluid problem.

#### **4.4 ADVANTAGES OF CFD OVER EXPERIMENTAL METHODS**

Conducting a CFD analysis can significantly reduce both the lead time and cost of developing a new design. This method offers the ability to examine complex systems where controlled experiments are challenging or impossible to carry out, such as very large systems or hazardous environments. Additionally, CFD analysis provides an abundance of highly detailed results. Compared to conducting physical experiments, which require facility rental and man-hour costs that increase with the number of data points and configurations tested, CFD codes generate large volumes of results at a negligible added cost. As a result, it is cost-effective to perform parametric studies, like optimizing equipment performance.

#### **4.5 WORKING OF A CFD CODE**

CFD codes are structured around numerical algorithms that can tackle fluid flow problems. To provide easy access to the solving power, all commercial CFD packages (Phoenics, Flow3D, and Star CD) include sophisticated user interfaces to input problem parameters and to examine the results. All codes contain 3 main elements.

- Pre-Processor
- Solver
- Post-Processor

##### **4.5.1 Pre-processor**

Pre-processing consists of the input of a flow problem to a CFD program using an operator-friendly interface and the subsequent transformation of this input into a form suitable for use by the solver. The user activities at the pre-processing stage involves,

- Definition of the geometry of the region of interest: the computational domain.
- Grid generation: the sub-division of the domain into several smaller, non- overlapping sub-domains known as a grid of cells or mesh (control volumes or elements).

- Selection of the physical and chemical phenomena that need to be modeled.
- Definition of fluid properties.
- Specification of appropriate boundary conditions at cells that coincide with or touch the domain boundary.

The solution to a flow problem is defined at the nodes inside each cell. The accuracy of a CFD solution is governed by the number of cells in each grid.

#### **4.5.2 Solver**

There are three distinct streams of numerical solution techniques: finite difference, finite element, and spectral methods. In outline, the numerical methods that form the basis of the solver perform the following steps.

- Approximation of the unknown flow variables using simple functions.
- Discretization by substitution of the approximations into the governing flow equations and subsequent mathematical manipulations.
- Solution of the algebraic equations.

The main differences between the three separate streams are associated with how the flow variables are approximated and with the discretization processes.

#### **4.5.3 Post-processor**

As in pre-processing a huge amount of development work has recently taken place in the post-processing field. With the increased popularity of engineering workstations, many of which have outstanding graphics capabilities, the leading CFD packages are now equipped with versatile data visualization tools. These include,

- Domain geometry and grid display.
- Vector plots.
- Line and shaded contour plots.
- 2D and 3D surface plots.
- Particle tracking.

- View manipulation (translation, rotation, scaling, etc.).
- Colour postscript output..

## 4.6 CFD CALCULATION

CFD is applied by first dividing or discretizing the geometry of interest into several computational cells. Discretization is the method of approximating the differential equations by a system of algebraic equations for the variables at some set of discrete locations in space and time. The discrete locations are referred to as the grid or the mesh. The continuous information from the exact solution of the Navier-Stokes partial differential equations is now replaced with discrete values. The number of cells can vary from a few thousand for a simple problem to millions for very large and complicated ones. Cells have a variety of shapes. Triangular and quadrilateral cells are generally used in 2D problems.

For 3D problems, hexahedral, tetrahedral, pyramidal, and prismatic-shaped cells can be used. In the past, CFD codes required the use of structured grids containing one cell type, such as brick-shaped hexahedral elements, in which the cells were positioned in regular patterns. Current codes allow cells to be located in an irregular, unstructured pattern, giving much greater geometric flexibility. Additionally, a good CFD code can accept grids consisting of a combination of different cell types, or hybrid grids, to address complex geometries, providing flexibility to the CFD analyst. Geometries are often created using computer-aided design (CAD) software. The geometry, either a wire frame or solid model is exported to the grid-generation software program to create the CFD quality grid. A few packages have combined both functions of CAD geometry creation and mesh generation into a single interface. With the grid created, the boundary conditions such as pressures, velocities, mass flows, and scalars specified, and physical properties defined, the CFD calculations can start.

The CFD codes will solve the appropriate conservation equations for all grid cells using an iterative procedure. Typical chemical process applications involve solving for mass conservation (using a continuity equation), momentum (using Navier Stokes equations), enthalpy, turbulent kinetic energy, turbulent energy dissipation rate, chemical species concentrations, and local reaction rates, and local volume fractions for multiphase problems. There are many commercial CFD packages for modeling and analyzing system involving fluid

flow, heat transfer, and associated phenomena such as chemical reactions. Some popular CFD packages include FLUENT, CFX, PHOENICS, and ANSYS. All these commercial CFD codes contain three main elements: Pre-processor, Solver, and Post-processor. This study concentrates on the use of the ANSYS 2022 R1 software package to simulate the flow and mixing behaviour, especially for chemical and thermal industrial applications.

## CHAPTER 5: NUMERICAL STUDY ON HEAT TRANSFER

It has been realized from the literature that changes in orifice number and frequency of the jet have a major influence on the heat transfer distribution along the target surface. This chapter deals with the numerical study on the heat transfer and flow characteristics of synthetic jet impingement cooling using multiple orifice. Numerical studies have been carried out using finite volume based software ANSYS 2022 R1. The numerical scheme is validated by comparing the results obtained from the published experimental work[1] The software used for the purpose is a finite volume based software package Ansys fluent. The numerical analysis under transient condition is conducted to examine the effect of frequency, Strouhal number and Reynolds number on the heat transfer characteristics of synthetic jet.

### 5.1 GEOMETRIC MODEL

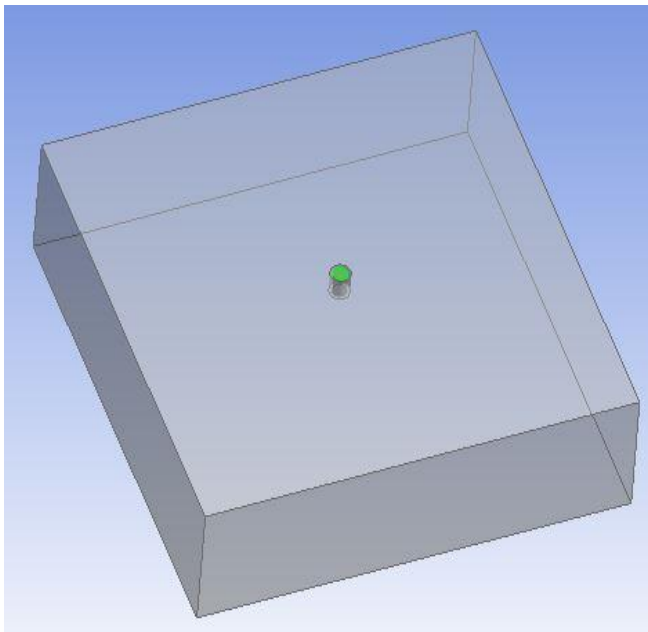


Fig.5.1(a) Geometry with orifice plate A

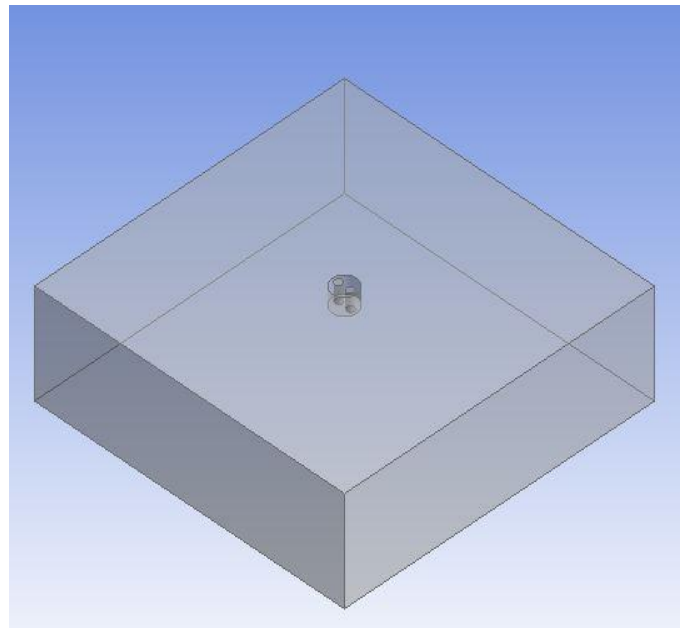


Fig.5.1 (b) Geometry with orifice plate B

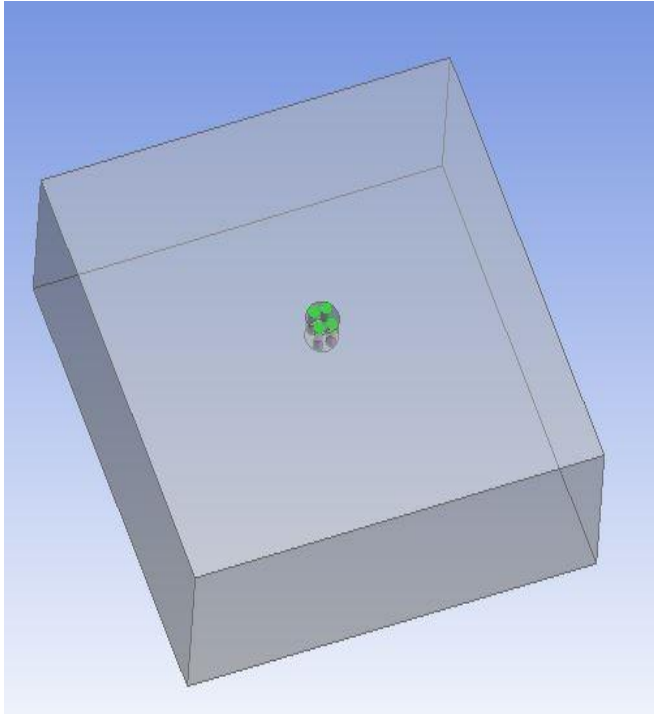


Fig.5.1(c) Geometry with orifice plate C

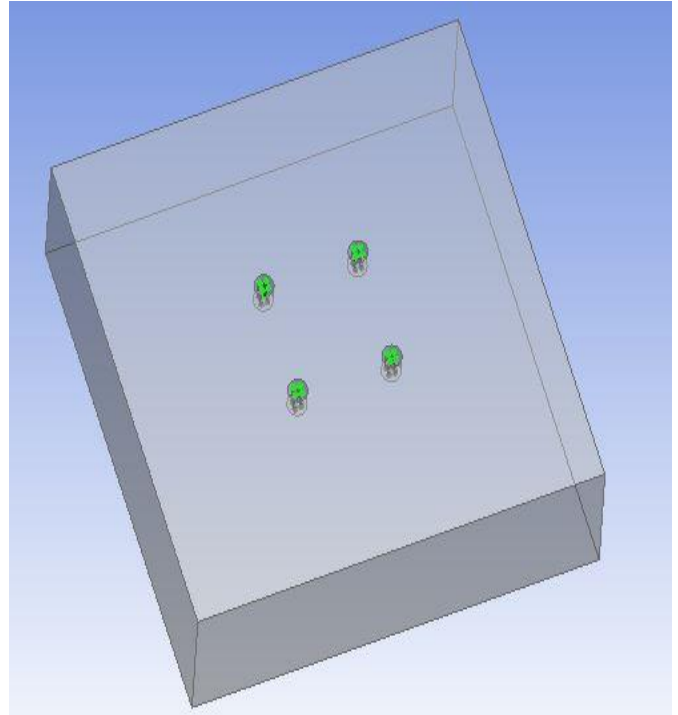


Fig.5.1 (d) Geometry with orifice plate D

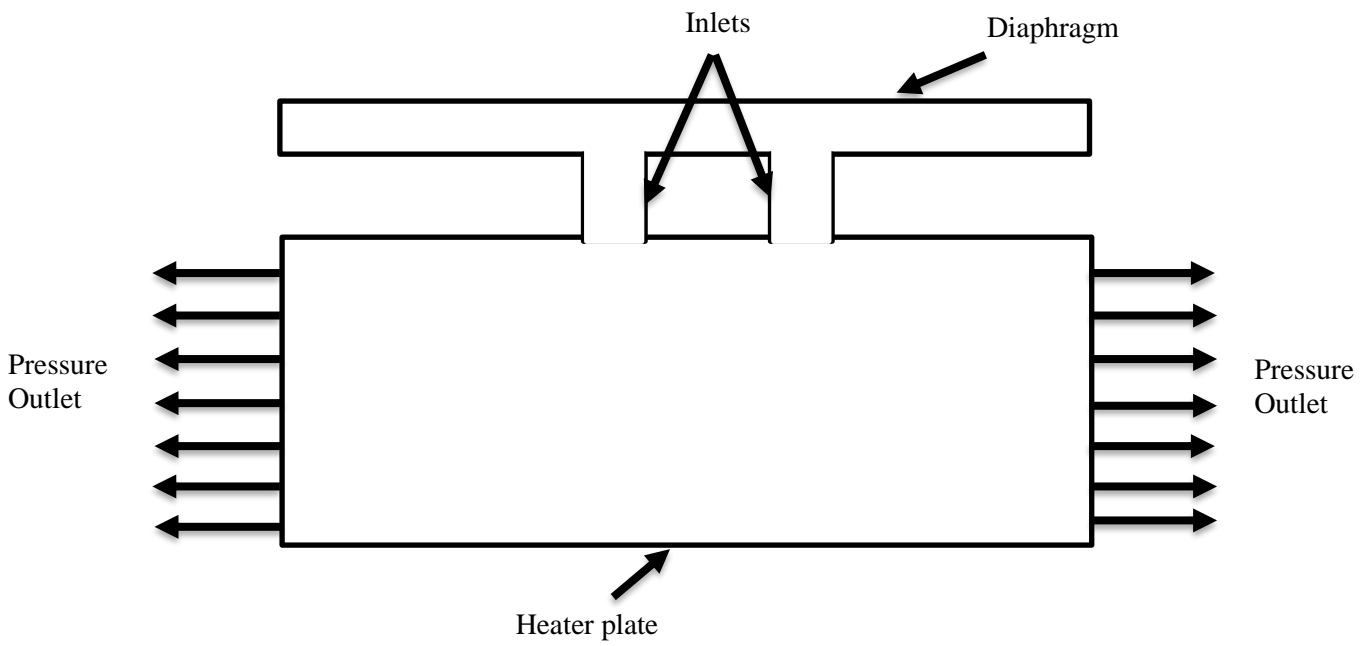


Fig.5.1 (e) 2D Computational Domain

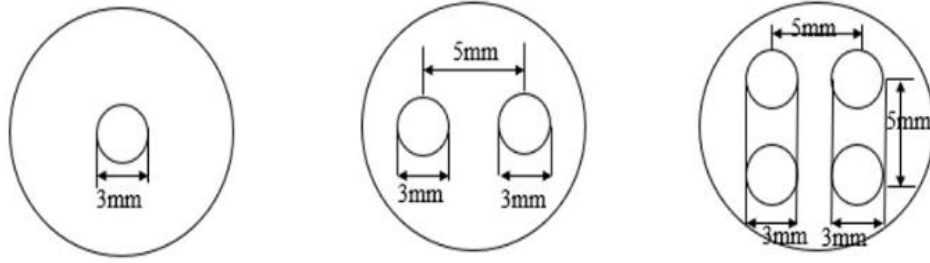


Fig.5.1(f) Plates with orifices of 3mm diameter.

Fig.5.1. Geometric model and orifice plates.

Modelling of the Synthetic jet impingement was carried out with a flat plate of dimension 130 X 130mm. The orifice is placed on a flat plate which is 24mm away from the target plate to be cooled. The orifice plate contains an orifice with 3mm diameter. Four different cases are studied by changing the number of orifices as shown in Figs.5.1 (a) to (f) and Table 5.1 respectively. The geometrical sketch in 2D of SJ impingement is shown in Fig 5.1(e).

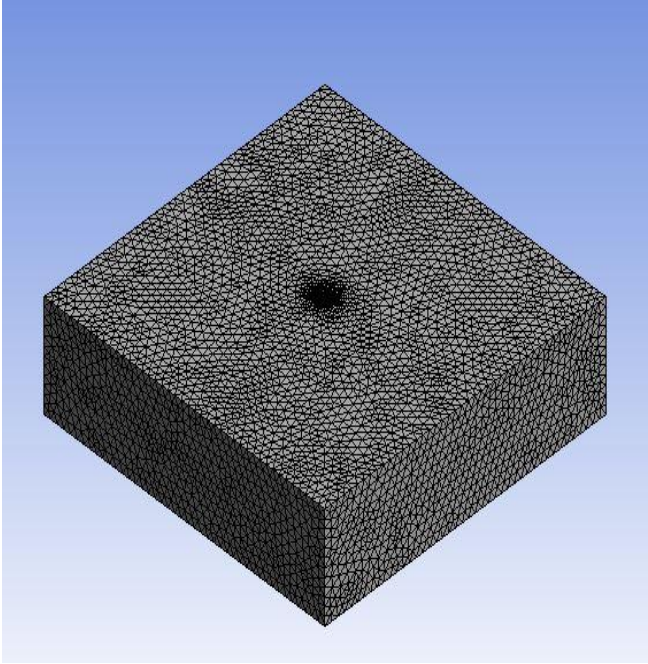
**Table 5.1:** Various Plates with Number of Orifices

Orifice Plates	Orifice diameter	Number of Orifices
Plate A	3mm	1
Plate B		2
Plate C		4
Plate D		16

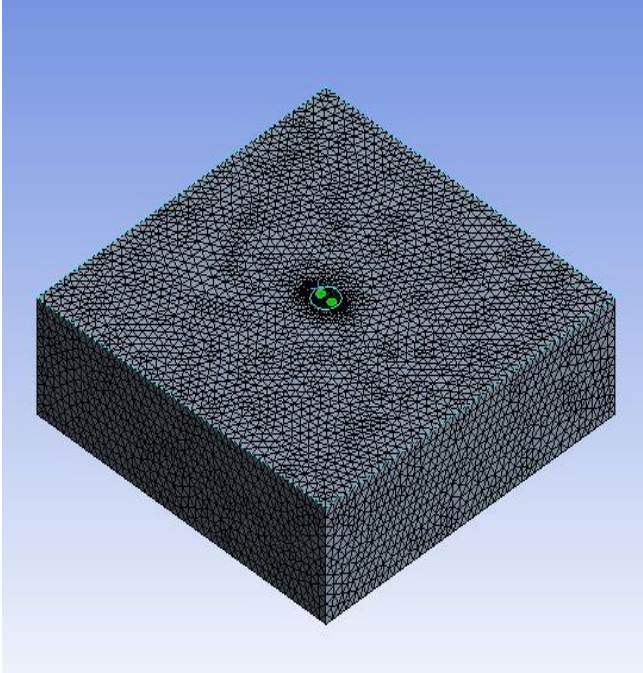
## 5.2 GRID GENERATION

Three-dimensional discretized model of Synthetic jet impingement was generated in ANSYS 2022 R1 in the pre-processor phase. Since the type of grids has bearing on the simulation results, in this study, the entire geometry is discretized into finite volume of tetrahedral grids to determine heat transfer and flow characteristics of synthetic jet impingement cooling using multiple orifice. Fig. 5.2,(a) to (d) shows the domain mesh for each geometry considered.

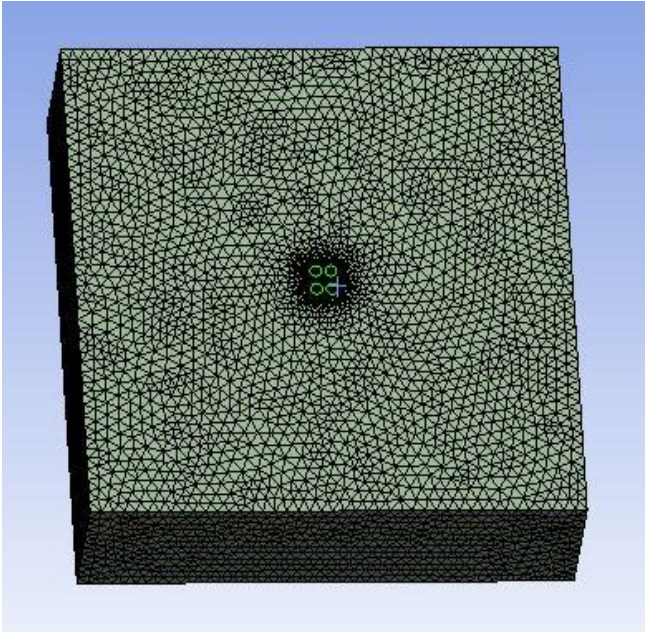
The size of mesh also greatly influences the result of any numerical simulation, therefore, the mesh independency test was carried out for different sizes of mesh as illustrated in Table 5.2.



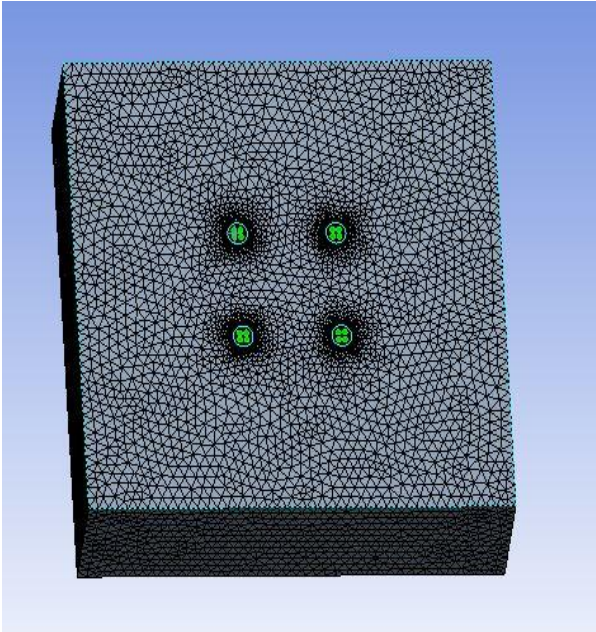
(a) Mesh with Orifice Plate A



(b) Mesh with Orifice Plate B



(c) Mesh with Orifice Plate C



(d) Mesh with Orifice Plate D

**Fig 5.2 :** The mesh of domain, (a) Mesh with Orifice Plate A (b) Mesh with Orifice Plate B  
(c) Mesh with Orifice Plate C (d) Mesh with Orifice Plate D.

**Table 5.2:** The effect of mesh size on the obtained results

<b>Applied Design</b>	<b>Mesh Size(m)</b>	<b>Mesh elements</b>	<b>Avg. Nusselt number</b>
<b>Plate A</b>	0.0008	86325	40.36
	0.0005	166299	41.78
	0.0003	234261	41.95
<b>Plate B</b>	0.0008	89779	41.04
	0.0005	183016	44.15
	0.0003	206725	43.99
<b>Plate C</b>	0.0008	97608	41.19
	0.0005	197004	43.94
	0.0003	223891	44.50
<b>Plate D</b>	0.0008	98976	42.55
	0.0005	203669	43.37
	0.0003	223865	45.74

As it is evident, the accuracy of the obtained results does not increase significantly with a notable growth in the size of mesh used for domain discretization. Therefore, the mesh with lower size was applied in all studied cases that will significantly reduce the computation time. The semi implicit method for pressure linked equation (SIMPLE) algorithm is employed for the purpose of pressure-velocity coupling.

Here, the analysis were conducted for a mesh size of 0.0005m with mesh elements of 166299 for plate A, 183016 for plate B, 197004 for plate C and 203669 for plate D. By these type of mesh configuration the reverse flow is minimized compare to other configurations and better smoothening is achieved. Also, convergence criteria can be obtained with minimum run time of the analysis.

### 5.3 FLUENT ANALYSIS

The synthetic jet heat and mass transmission process is thought to be unstable, two-dimensional, incompressible, turbulent, and to have consistent physical characteristics. Based on those simplifications above, the governing equations in terms of RANS (Reynolds Averaged Navier–Stokes) of this work are written as,

$$\frac{\partial \bar{u}_i}{\partial x_i} = 0 \quad (5.3.1)$$

$$\rho \left( \frac{\partial \bar{u}_i}{\partial t} + \frac{\partial \bar{u}_i \bar{u}_j}{\partial x_j} \right) = -\frac{\partial \bar{p}}{\partial x_i} + \frac{\partial}{\partial x_i} \left[ \mu \left( \frac{\partial \bar{u}_i}{\partial x_j} + \frac{\partial \bar{u}_j}{\partial x_i} \right) - \overline{\rho u'_i u'_j} \right] \quad (5.3.2)$$

$$\frac{\partial T}{\partial t} + u_j \frac{\partial T}{\partial x_j} = \alpha \frac{\partial}{\partial x_j} \frac{\partial T}{\partial x_j} - \frac{\partial \overline{u'_j T'}}{\partial x_j} \quad (5.3.2)$$

where the term of  $-\overline{\rho u'_i u'_j}$  represents the Reynolds stresses.

#### Continuity Equation

$$\frac{\partial u}{\partial x} + \frac{\partial v}{\partial y} + \frac{\partial w}{\partial z} = 0$$

The x-component of the momentum equation is

$$\rho \frac{Du}{Dt} = \frac{\partial(-p + \tau_{xx})}{\partial x} + \frac{\partial \tau_{yx}}{\partial y} + \frac{\partial \tau_{zx}}{\partial z} + S_{Mx}$$

The y-component of the momentum equation is

$$\rho \frac{Dv}{Dt} = \frac{\partial \tau_{xy}}{\partial x} + \frac{\partial(-p + \tau_{yy})}{\partial y} + \frac{\partial \tau_{zy}}{\partial z} + S_{My}$$

The z-component of the momentum equation is

$$\rho \frac{Dw}{Dt} = \frac{\partial \tau_{xz}}{\partial x} + \frac{\partial \tau_{yz}}{\partial y} + \frac{\partial(-p + \tau_{zz})}{\partial z} + S_{Mz}$$

The Navier-Stokes equation is obtained by substituting the shear stress components in the momentum equations. The Navier-Stokes equation can be written in a beneficial form as follows.

$$\begin{aligned}\rho \frac{Du}{Dt} &= -\frac{\partial p}{\partial x} + \text{div}(\mu \text{grad } u) + S_{Mx} \\ \rho \frac{Dv}{Dt} &= -\frac{\partial p}{\partial y} + \text{div}(\mu \text{grad } v) + S_{My} \\ \rho \frac{Dw}{Dt} &= -\frac{\partial p}{\partial z} + \text{div}(\mu \text{grad } w) + S_{Mz}\end{aligned}$$

### 5.3.1 Boundary Conditions

It is assumed that the flow is turbulent and incompressible in three dimensions. Consideration is given to how temperature affects a fluid's density, viscosity, and thermal conductivity. SST k- $\omega$  turbulence model is the one employed. While the k- $\omega$  model focuses on the aspect, in the case of an impinging target surface, the impacts in the near-wall region should be considered. Additionally, the shear stress transport k- $\omega$  (SST/ k- $\omega$ ) model is used to strike a balance between computational efficiency and accuracy.

For an accurate solution to a fluid flow problem, it is crucial to define the appropriate boundary types and boundary conditions. While some boundary conditions are set by simulation software, the majority are defined by physical phenomena. The inlet air temperature is given as 300k and the inlet jet velocity is given corresponding to the Reynolds number. A constant net heat flux of 4000W/m<sup>2</sup> is applied to the bottom surface of the target plate and all other wall surfaces are assumed to be adiabatic. The jet velocity is defined as a User defined function(UDF) which is in the form of a sinusoidal function of frequency of the vibrating diaphragm.

Velocity inlet as UDF is applied at the jet inlet as described,

```
#include "udf.h"
DEFINE_PROFILE(unsteady_velocity, thread, position)
{
    face_t f;
    real t = CURRENT_TIME;

    real vel;
    vel= 50*sin(2*3.14*f*t);
    begin_f_loop(f, thread)
    {
        F_PROFILE(f, thread, position) = vel;
    } end_f_loop(f, thread)
}
```

### 5.3.2 Input Parameters

Certain parameter values, such as material qualities and beginning parameter values must be entered as input parameters into the CFD tool. The table contains the values for the input parameters.

<b>Table 5.3 Input parameters</b>		
<b>Function</b>	<b>Specifications</b>	
Solver	Energy	On
	Type	Pressure-based
	Time	Transient
	Viscous model	SST- k-omega model
Materials	Solid	Copper
	Fluid	Air

### **5.3.3 Solution Technique**

A discretization strategy is needed to solve the governing equations and scalar variables like temperature. For this work, two discretization schemes are used,

A stable solution is provided by the First Order upwind solution method, which also exhibits a good rate of residual convergence. This plan's drawback is that the solution's accuracy could not be adequate. Therefore, where great precision is not the primary objective, the first order upwind technique can be employed. The Second Order upwind approach, on the other hand, delivers extremely precise simulation results. However, the amount of time needed for the simulation increases significantly when the second order upwind solution technique is used. Therefore, first order upwind solution method was used in the current study by taking into account for the calculation capability and the time available.

### **5.3.4 Convergence Criteria**

The solution's convergence is determined by the difference in required parameter i.e., Nusselt number value after each iteration. Convergence criteria are established under the presumption that the solution would remain unchanged after convergence. One approach to the problem is the pressure-velocity coupling, which employs the SIMPLE system. The parameters were set in Fluent, and then the solution was initialized. Depending on how easily the convergence occurred and how long it took to obtain the results, iterations were performed.

## CHAPTER 6: EQUATIONS AND NUMERICAL CALCULATIONS

The Reynolds number is defined as the following equation,

$$\mathbf{Re} = \frac{\rho U_0 D}{\mu} \quad (6.1)$$

Where;

$\rho$  - density of fluid, kg/m<sup>3</sup>

$U_0$  – velocity of fluid, m/s

$D$  – Hydraulic diameter of orifice, m

$\mu$  - Dynamic viscosity of fluid, kg/ms

The Nusselt number is defined as,  $\mathbf{Nu(x,t) = hD/k}$  (6.2)

Where;

$h$ -heat transfer coefficient, W/m<sup>2</sup>K

$D$ -the diameter of the orifice,m

$k$  is the thermal conductivity of the fluid, W/mK.

The average velocity,  $\mathbf{U_0 = f. \int_0^T u(t)dt = \frac{1}{T} . \int_0^T u(t)dt}$  (6.3)

where  $T$  symbolizes the whole period whereas the integral interval is only the ejection phase; the integral is defined as the stroke length.

Time-area averaged Nusselt number( $Nu_{avg}$ ) is used to estimate the mean heat transfer effect among the whole heated region. which is defined as,

$$\mathbf{Nu_{avg} = \frac{1}{\Delta t} \frac{1}{\Delta x} \int_0^T \int_0^{L/2} Nu(x, t) dx dt} \quad (6.4)$$

where  $L$  stands for the length of whole target wall;  $L/2$  represents the length of heated region.

Similarly, the area-averaged Nusselt number  $Nu_A$  is represented by,

$$\mathbf{Nu_A(t) = \frac{1}{\Delta x} \int_0^{L/2} Nu(x, t) dx} \quad (6.5)$$

Strouhal number or Reciprocal of stroke length,  $St = \frac{fD}{U_0} = \frac{D}{L_0}$  (6.6)

Convective heat transfer coefficient,  $h = \frac{Q}{A(T_1 - T_a)} \frac{W}{m^2k}$  (6.7)

Where,  $Q$  =input power (W)  
 =VI  
 V =Voltage (V)  
 I =Current (A)  
 $T_1$  =Temperature of top surface (°C)  
 $T_a$  =Ambient Temperature (°C)

Heat Flux,  $q = Q/A$   
 $q = W/m^2$   
 A =Area (m<sup>2</sup>)

## CHAPTER 7: RESULTS AND DISCUSSION

In this chapter the numerical results are presented for the heat transfer and flow characteristics of synthetic jet impingement cooling. The average Nusselt number is considered for the evaluation of the performance of the synthetic jet impingement. In this study, the heat transfer characteristics of synthetic jet impingement cooling with multiple orifice (2,4 and 16 orifices) were analysed with different operating frequencies ( $f=1\text{Hz}$  to  $f=5\text{Hz}$  and  $f=100\text{Hz}$  to  $f=500\text{Hz}$ ) with different Reynolds numbers ( $Re=10000$  to  $20000$ ) as well as Strouhal numbers ( $St=0.006$  to  $St=0.030$ ).

### 7.1 MESH INDEPENDENT STUDY

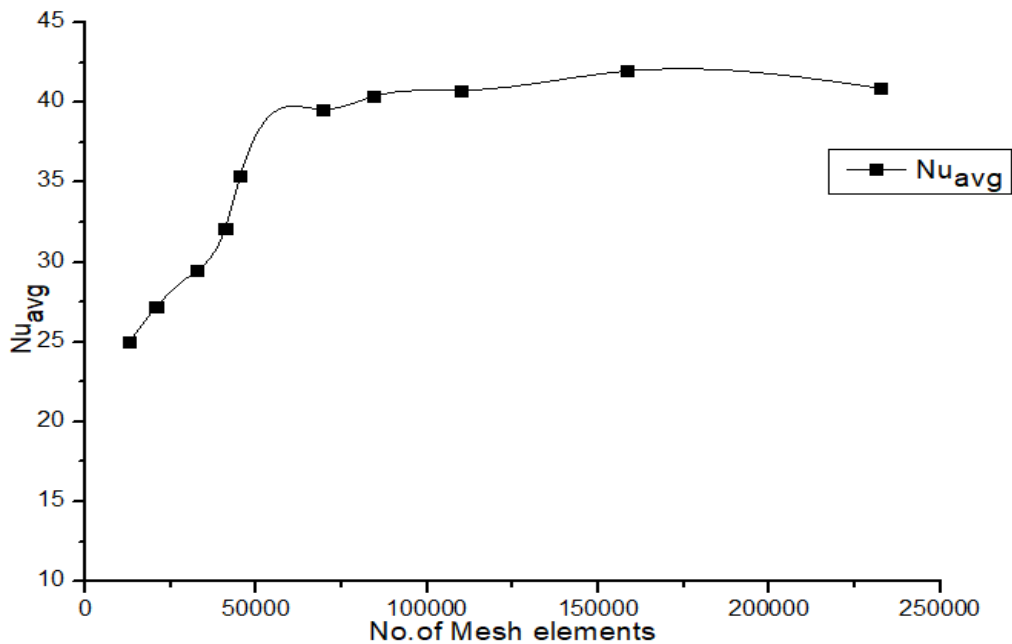


Fig. 7.1 Variation of average Nusselt number with No. of elements

The number of mesh elements in the various cases are 12916, 20701, 32532, 40857, 45259, 69383, 84349, 109688, 158271, 232429. By comparing with the ninth and tenth mesh configuration in terms of Nusselt number, the variation is relatively less.

## 7.2 VALIDATION OF NUMERICAL RESULTS

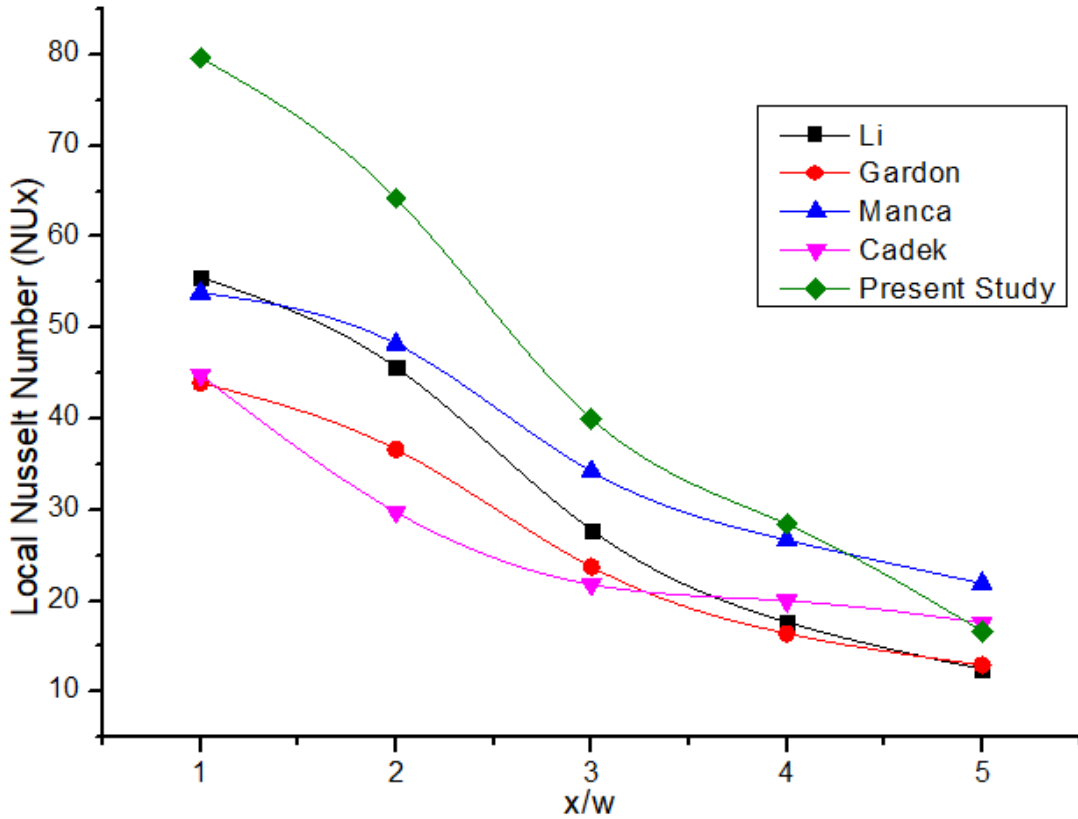


Fig. 7.2 Validation of Present study with References.

The validation is conducted via comparing present results with numerical investigations by Ping- Li et al.[1], Manca et al. [11] and experimental ones provided by Gardon and Akfirat [10] as well as Cadek [9] , in the same condition of  $Re = 11000$ ,  $Z/D = 6$ . The graph shows 15% variation between present model and reference. As shown in Fig. 5.2, the current results are in great consistency with those of literatures close to the stagnation point. Especially, they exhibit better approximation to experimental results in the region of  $x/w > 2$  than those of Manca et al. [11] . Therefore, the proposed model in present work is regarded as reliable judging from the comparison results, and further numerical analyses are to be conducted based on this validated model. The validated data is shown in fig.7.2.

**Table 7.1 Validation-Values of local Nusselt number**

<b>x/w</b>	<b>Ping Li</b>	<b>Gardon</b>	<b>Manca</b>	<b>Cadek</b>	<b>Present Study</b>
1	55.6	43.94	53.83	44.81	79.63
2	45.64	36.64	48.22	29.76	64.23
3	27.79	23.74	34.24	21.78	40
4	17.67	16.403	26.68	20	28.41
5	12.48	12.95	21.91	17.603	16.67

### **7.3 EFFECT OF HIGH AND LOW FREQUENCIES ON AVERAGE NUSSELT NUMBER**

The frequencies varies from 1Hz to 5Hz in the range of 1Hz and from 100Hz to 500Hz in the range of 100Hz. For all these frequencies, studies have been conducted by varying the Reynolds number from 10000 to 20000 in the range of 5000. Fig.7.3 (a), (b) and (c) shows the variation of Nusselt number at the top surface of the heater plate for multi orifices with different frequencies for different Reynolds number.

#### **7.3.1 Variation of average Nusselt number with High Frequencies at Re=20000 and diameter of the orifices 3mm.**

Numerical simulation was conducted by varying the frequencies from 100Hz to 500Hz for different orifice plates (Plates A,B,C and D) of orifice diameter 3mm. The number of orifices varies in the orifice plates as 1,2,4 and 16 numbers.

Fig.7.3.(a) shows the variation at Re=20000 for different plates. It is seen that the Plate D with 16 orifices shows more increase in Nusselt number which means that it shows better heat transfer performance compared to other plates.. The variation for Plates A, B and C is similar for all Reynolds numbers.

#### **7.3.2 Variation of average Nusselt number with High Frequencies at Re=15000 and diameter of the orifices 3mm.**

Fig.7.3.(b) shows the variation at Re=15000 for different plates. The variation of increase in average Nusselt number is low as compared to Re=20000 which means the rate of change of heat transfer is low as compared to Re=20000. Also, similar variation can be seen for Plates A, B and C.

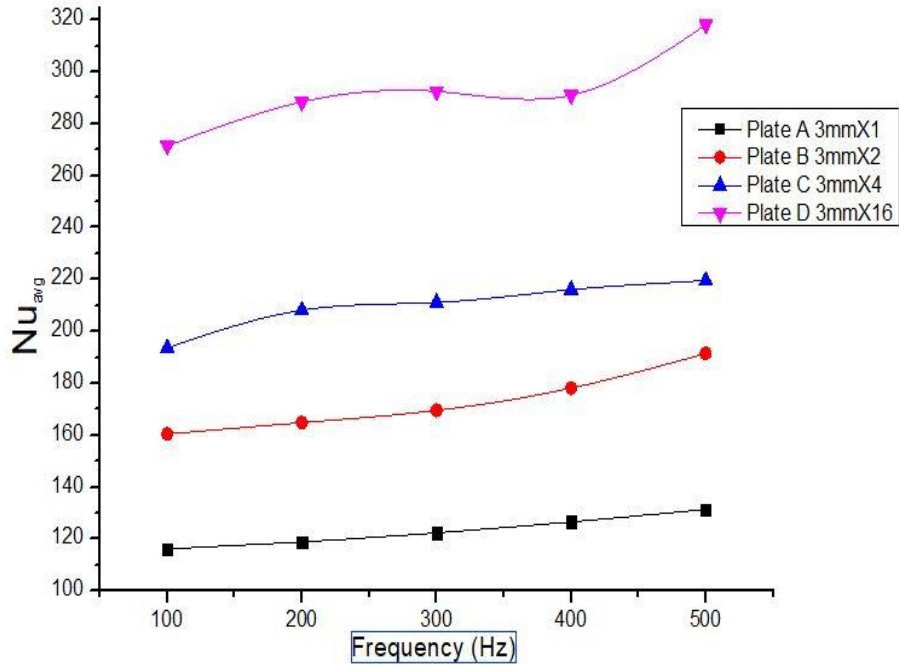


Fig.7.3.(a) Variation of  $Nu_{avg}$  with high frequencies at  $Re=20000$ .

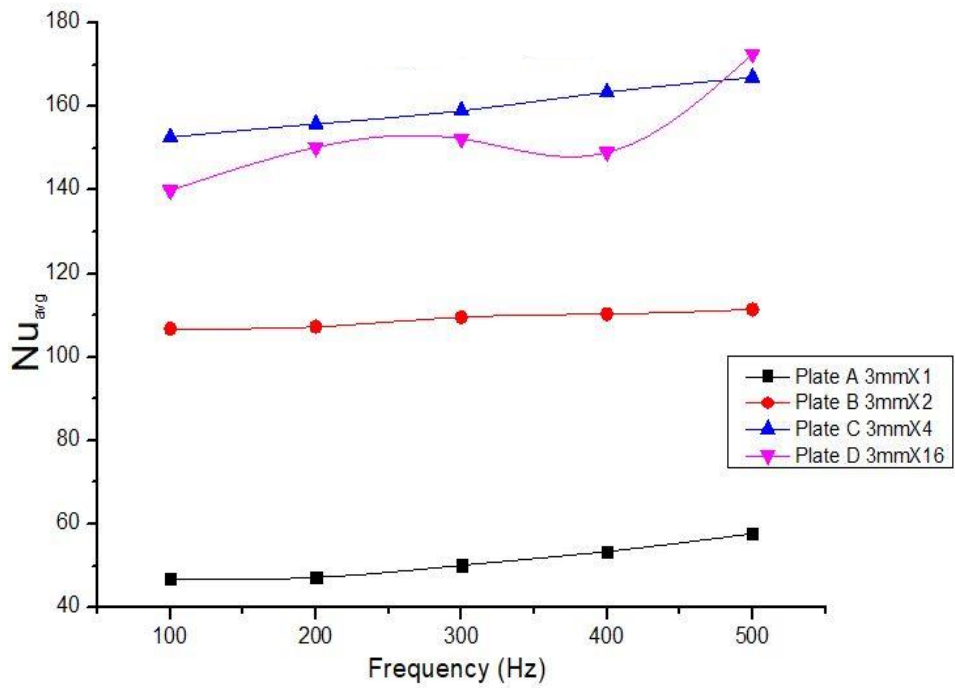


Fig.7.3.(b) Variation of  $Nu_{avg}$  with high frequencies at  $Re=15000$ .

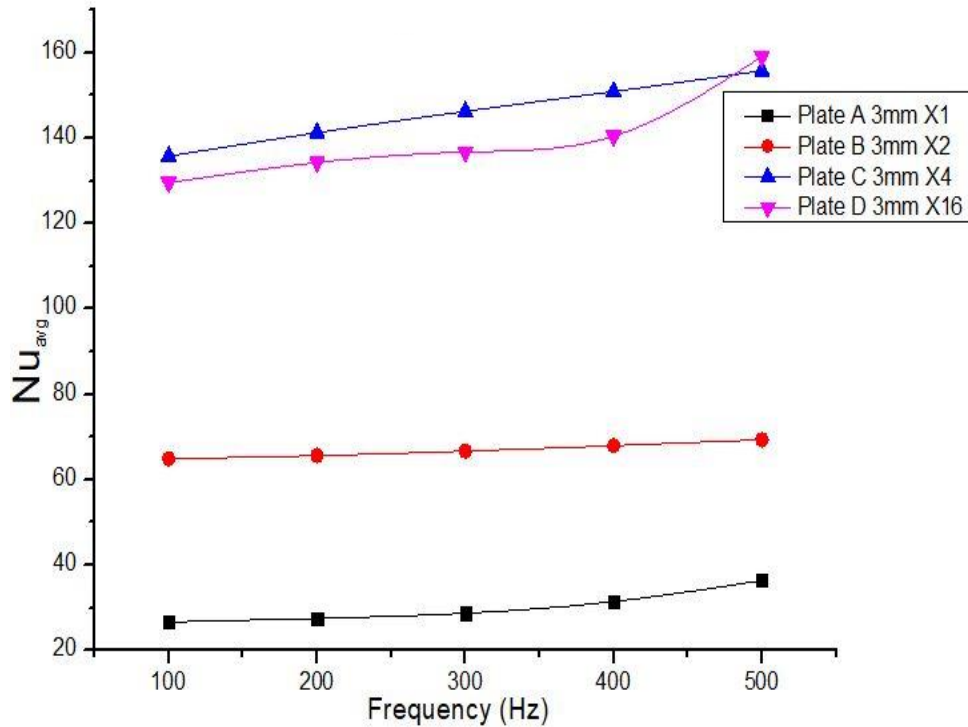


Fig.7.3.(c)Variation of  $Nu_{avg}$  with high frequencies at  $Re=10000$ .

### 7.3.3 Variation of average Nusselt number with High Frequencies at $Re=10000$ and diameter of the orifices 3mm.

Fig.7.3.(c) shows the variation at  $Re=10000$  for different plates. The variation of increase in average Nusselt number is low as compared to  $Re=20000$  and  $Re=15000$  which means the rate of change of heat transfer is low as compared to the other two cases. Also, similar variation can be seen for all plates at  $Re=15000$  and  $Re=10000$ . Compared to  $Re=15000$ , the variation of increasing in average Nusselt number is relatively less.

### 7.3.4 Conclusion from the High frequency analysis

From the analysis, it is found that the average Nusselt number increases with increasing frequency (100Hz to 500Hz) for a constant Reynolds number. But for plate D similar variation can be observed for all selected range of Reynolds number. For the plate D, the frequency changes from 100Hz to 500Hz, then the average Nusselt number increases from 129.53 to 159.04 for  $Re=10000$ , from 139.84 to 172.58 for  $Re=15000$  and from 271.51 to 318.14 for  $Re=20000$ . In all cases, there was some reverse flow occurs in some faces (2 to 23 faces) of the meshed geometry in a short interval of time.

### 7.3.5 Variation of average Nusselt number with Low Frequencies and diameter of the orifices 3mm.

Numerical simulation was conducted by varying the frequencies from 1Hz to 5Hz for different orifice plates (Plates A,B,C and D) of orifice diameter 3mm. The number of orifices varies in the orifice plates as 1,2,4 and 16 numbers.

Fig.7.3.(d) shows the variation at  $Re=20000$  for different plates. From the analyses, initially the heat transfer rate is low for plate D compared with plate C. As the frequency increases the average Nusselt number also increases for plates. The Plate D with 16 orifices shows more increase in Nusselt number which means that it shows better heat transfer performance compared to other plates. Similar trendlines can be seen at other Reynolds numbers( $Re=15000$  and  $Re=10000$ ) which are represented graphically in Fig.7.3.(e) and Fig.7.3.(f).

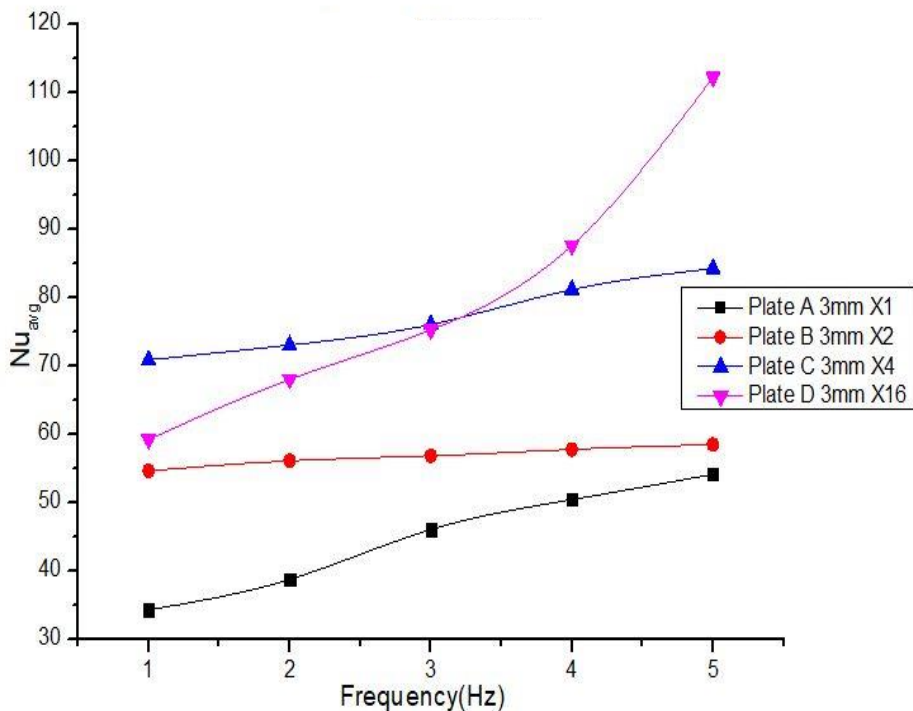


Fig 7.3.(d) Variation of  $Nu_{avg}$  with low frequencies at  $Re=20000$ .

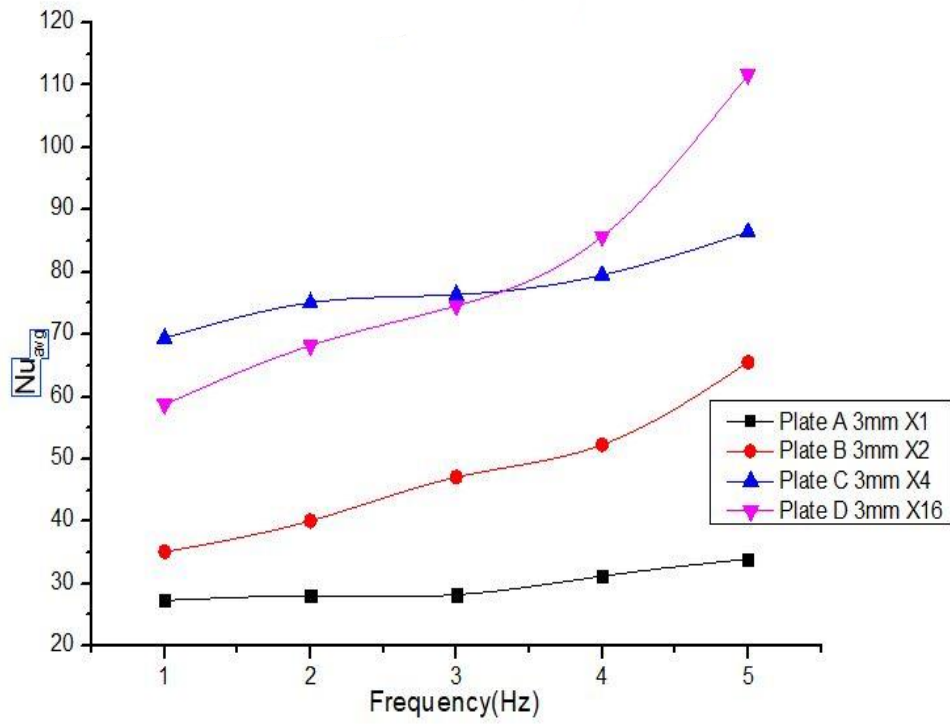


Fig 7.3.(e) Variation of  $Nu_{avg}$  with low frequencies at  $Re=15000$ .

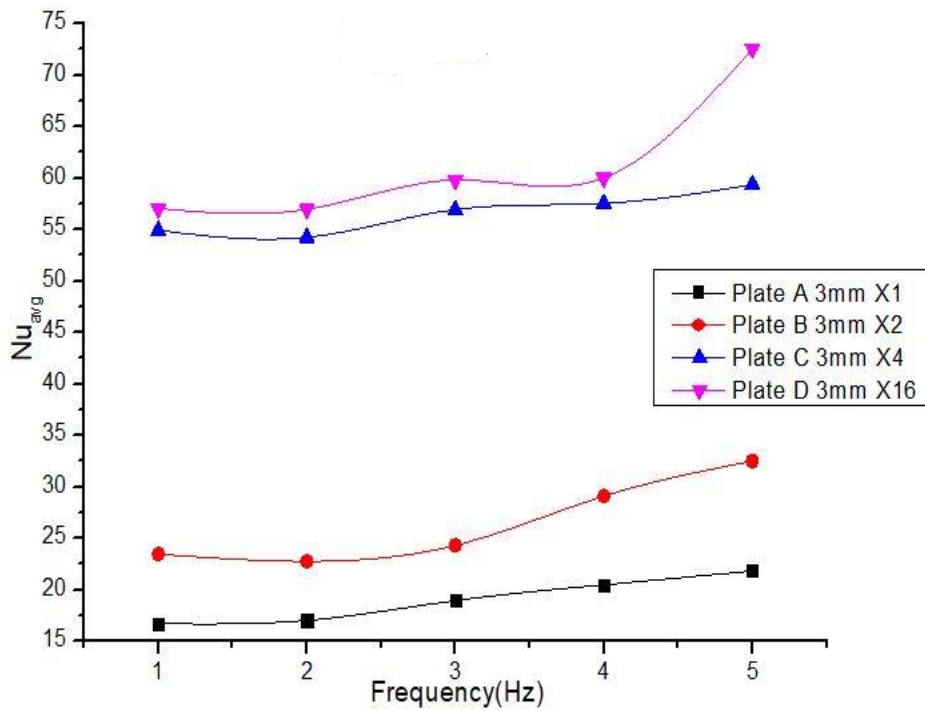


Fig 7.3.(f) Variation of  $Nu_{avg}$  with low frequencies at  $Re=10000$ .

Fig.7.3 Variation of  $Nu_{avg}$  with High and Low frequencies.

### 7.3.6 Conclusion from the Low frequency analysis

From the analysis, it is found that the average Nusselt number increases with increasing frequency (1Hz to 5Hz) for a constant Reynolds number. For Plate D with 16 orifices shows more heat transfer capacity as compared to other plates. All other plates (A,B, and C) shows similar variation. Nonlinear variation trend between average Nusselt number and forcing frequency can be observed at each Reynolds number (Re= 10000 to Re=20000). In all cases, there was some reverse flow occurs in some faces (4 to 43 faces) of the meshed geometry in a short interval of time.

### 7.4 VARIATION OF LOCAL NUSSELT NUMBER ( $Nu_x$ ) IN RADIAL DIRECTION

Fig.7.4 shows the variation of  $Nu_x$  in the radial direction from the stagnation point for a 2 orifices synthetic jet. The maximum Nusselt number is obtained at the stagnation point i.e; the heat transfer rate is maximum at which the air jet hits directly on the plate. The rate of decrease in Nusselt number with radial distance depends on the Reynolds number of the flow. At low Reynolds numbers, the decrease in Nusselt number with radial distance is relatively slow, while at high Reynolds numbers, the decrease is much more rapid. The Nusselt number is highest at the center of the impingement region and decreases towards the periphery.

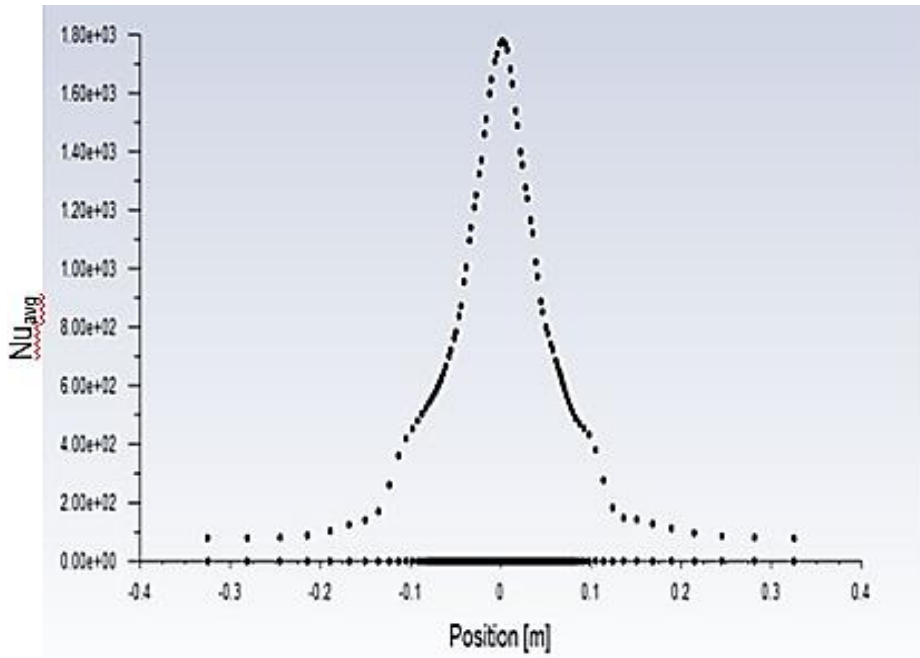


Fig. 7.4 Variation of  $Nu_{avg}$  in radial direction of the plate for 2 orifices.

Table 7.2 Range of studied parameters	
Parameters	Value
Frequency, f (Hz)	1,2,3,4,5,100,200,300,400,500
Reynolds number, Re	10000,15000,20000
Strouhal number, St	0.006,0.012,0.018,0.024,0.030,0.036

### 7.5 EFFECT OF REYNOLDS NUMBER ON HEAT TRANSFER

The average Nusselt number increases with Reynolds number by 5% as the Reynolds number increased from 10000 to 20000. As the Reynolds number increases, the turbulence level increases and the spreading of jet increases which resulting in a better heat transfer performance. Fig.7.5. shows the variation for Reynolds number with average Nusselt number. The correlation between average Nusselt number and Reynolds number is shown below.

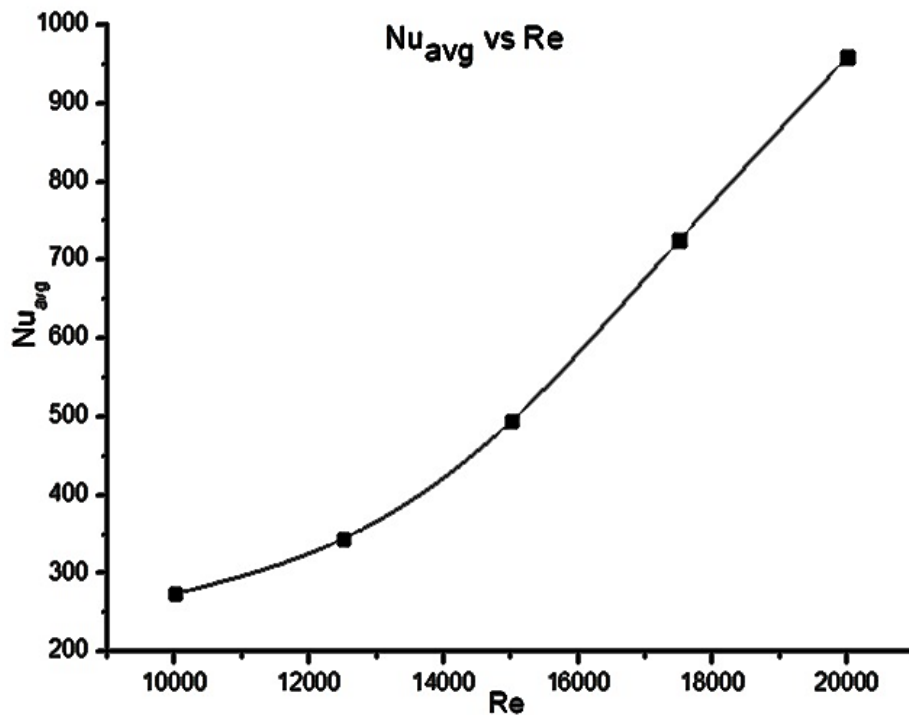


Fig. 7.5 Variation of average Nusselt number with Reynolds number.

$$Nu_{avg} = -4E-10(Re)^3 + 2E-05(Re)^2 - 0.3398(Re) + 1761.4.$$

The present polynomial has a high fitting precision shown in the graph with a  $R^2 = 0.9997$ .

An increase in Reynolds number leads to an increase in heat transfer due to the enhanced fluid mixing and turbulence induced by the synthetic jet flow. At low Reynolds numbers, the synthetic jet flow is laminar and has a low momentum transfer, resulting in a weak cooling effect. As the Reynolds number increases, the synthetic jet flow becomes turbulent, which enhances the mixing of the fluid and leads to a stronger cooling effect. However, at high Reynolds numbers, the synthetic jet flow can become unsteady, which may decrease the cooling effectiveness due to the fluctuation of the impinging jet.

## **7.6 DEPENDANCE OF HEAT TRANSFER ON NUMBER OF ORIFICES**

As compared with single orifice, multiple orifice exhibits a higher average Nusselt number. For multi orifice, the diameter of the orifice is maintained as 3 mm and the number of orifices varied as 2 and 4. Maximum heat transfer is obtained with a 3 mm orifice. The maximum average Nusselt number for 3 mm orifice diameter obtained at  $Z/D$  ratios of 8 [Arun Jacob et al.]. At  $Z/D$  ratio 2, there is less recirculation effect as compared with  $Z/D$  ratio 4. With the increase of  $Z/D$  ratio  $> 4$  there is an increase in the availability of fresh air and also the vortices achieve higher momentum. For a given frequency the jet velocity decreases with an increase in diameter of the orifice. At higher  $Z/D$  ratios the increase in diameter may cause a recirculation effect that will affect the heat transfer adversely.

The reason for higher heat transfer rate for multiple orifice is high mass flow rate and impingement of larger vortical structures [Chaudhari et al.]. Fig.5.1(f) shows the different orifice plates with number of orifices (1, 2 and 4). This is because more orifices produce a denser array of vortices, which enhances fluid mixing and heat transfer by breaking up the thermal boundary layer on the heated surface. Increasing the number of orifices in synthetic jet cooling generally results in a higher heat transfer coefficient due to the increased momentum transfer and enhanced mixing caused by the impinging jets. This is because more orifices produce a denser array of vortices, which enhances fluid mixing and heat transfer by breaking up the thermal boundary layer on the heated surface.

In summary, the number of orifices in synthetic jet cooling affects the heat transfer performance by influencing the flow structure, momentum transfer, and pressure drop. Increasing the number of orifices generally leads to a higher heat transfer coefficient, but it can also increase the pressure drop and pumping power requirements. Therefore, the optimal number of orifices needs to be determined based on the specific application and operating conditions.

## 7.7 EFFECT OF STROUHAL NUMBER ON HEAT TRANSFER

Generally, an increase in Strouhal number leads to an increase in heat transfer due to the enhanced mixing and momentum transfer induced by the synthetic jet flow. Fig.7.6. (a), (b) and (c) shows the variation of average Nusselt number with Strouhal number at various Reynolds numbers. At constant frequency, the average Nusselt number goes up as decrease in Strouhal number. Smaller Strouhal number can only be generated by larger Reynolds number. Also the stroke length decreases with frequency at constant Reynolds number. Turbulence kinetic energy increases as Strouhal number improves thus results more violent mixing thus get better cooling effect. Turbulence intensity dominates the heat transfer process, influenced by Strouhal number. At low Strouhal numbers, the synthetic jet flow is weak, and the heat transfer coefficient is relatively low. As the Strouhal number increases, the synthetic jet flow becomes stronger, and the heat transfer coefficient increases due to the enhanced fluid mixing and momentum transfer induced by the synthetic jet.

The present polynomials has a high fitting precision shown in Fig.7.6.(a),(b) and (c).

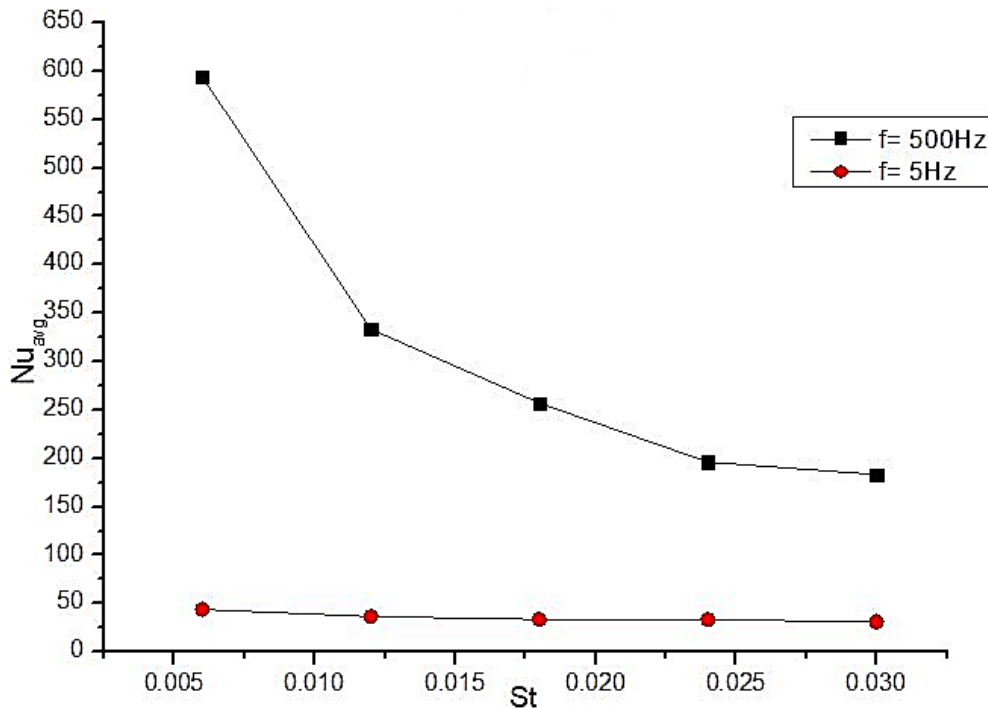


Fig.7.6(a) Variation of average Nusselt number with Strouhal Number for single orifice.

However, at high Strouhal numbers, the synthetic jet flow can become too strong, leading to flow separation, reduced heat transfer, and increased pressure drop. Therefore, there is an optimal Strouhal number that maximizes heat transfer while minimizing pressure drop. Numerical analysis shown that the heat transfer coefficient increases with increasing Strouhal number up to an optimum value and then begins to decrease.

In the range of Strouhal numbers from 0.006 to 0.030, the effect of the Strouhal number on heat transfer in synthetic jet impingement cooling can be studied. Experimental studies have shown that as the Strouhal number increases within this range, the heat transfer coefficient also increases due to the enhanced fluid mixing and momentum transfer induced by the synthetic jet flow[Carlo Salvatore Greco et al.]. At low Strouhal numbers ( $< 0.01$ ), the synthetic jet flow is weak, and the heat transfer coefficient is relatively low. As the Strouhal number increases, the synthetic jet flow becomes stronger, and the heat transfer coefficient increases due to the enhanced fluid mixing and momentum transfer induced by the synthetic jet. However, at very high Strouhal numbers ( $> 0.03$ ), the synthetic jet flow can become too strong, leading to flow separation, reduced heat transfer, and increased pressure drop.

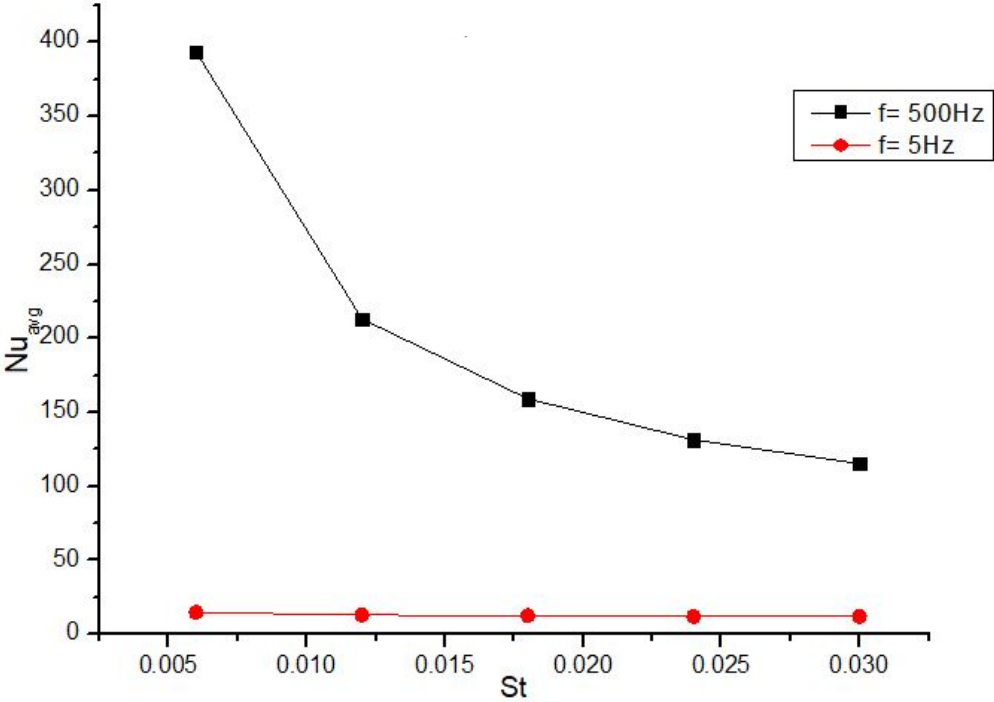


Fig.7.6(b)Variation of average Nusselt number with Strouhal Number for 2 orifices.

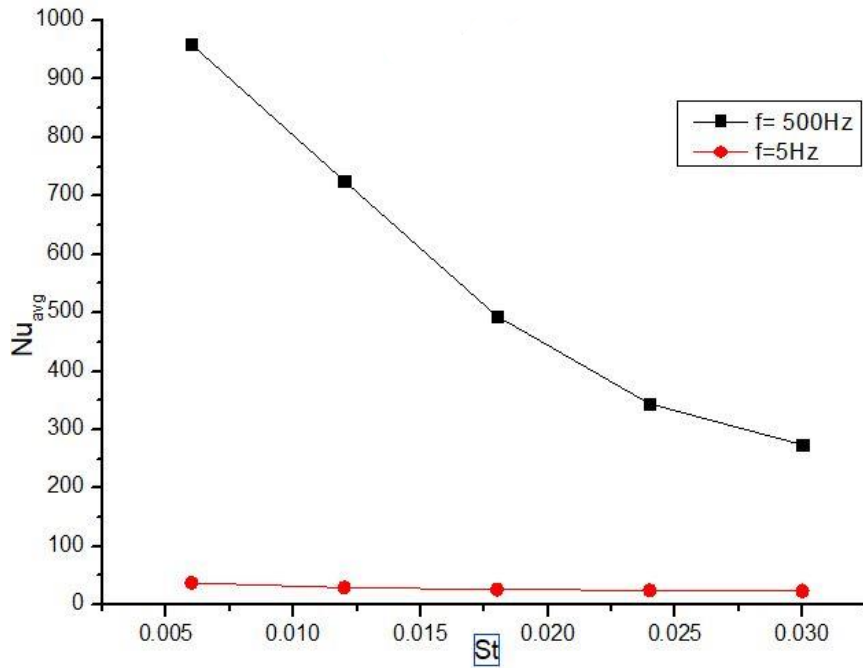


Fig.7.6(c) Variation of average Nusselt number with Strouhal Number for 4 orifices.

Fig.7.6. Variation of average Nusselt number with Strouhal Number.

Numerical simulations have also shown that within the range of Strouhal numbers from 0.006 to 0.030, there exists an optimal Strouhal number that maximizes heat transfer while minimizing pressure drop. This optimal Strouhal number can vary depending on the specific application, nozzle geometry, and operating conditions. In general, the optimal Strouhal number for maximum heat transfer is found to be in the range of 0.02-0.025.

In summary, within the range of Strouhal numbers from 0.006 to 0.030, the heat transfer performance of synthetic jet impingement cooling is highly dependent on the Strouhal number. As the Strouhal number increases within this range, the heat transfer coefficient generally increases due to the enhanced fluid mixing and momentum transfer induced by the synthetic jet flow. However, there exists an optimal Strouhal number that maximizes heat transfer while minimizing pressure drop, and this optimal Strouhal number can vary depending on the specific application and operating conditions. The Strouhal number plays a crucial role in determining the heat transfer performance of synthetic jet impingement cooling. A suitable range of Strouhal number should be selected to achieve optimal cooling effectiveness while avoiding undesirable flow instabilities and pressure drop.

## 7.8 EFFECT OF STATIC TEMPERATURE DISTRIBUTION

The static temperature distribution on the hot plate plays an important role in determining the heat transfer performance of synthetic jet cooling. The static temperature distribution on the hot plate affects the local heat transfer coefficient and the overall heat transfer rate. Fig.7.7. shows the shape of static temperature distribution at the impingement surface of the target plate with multiple orifice. The maximum heat transfer takes place at the stagnation point of the centre jet. The path lines of the air jet impingement is represented in Fig.7.8.

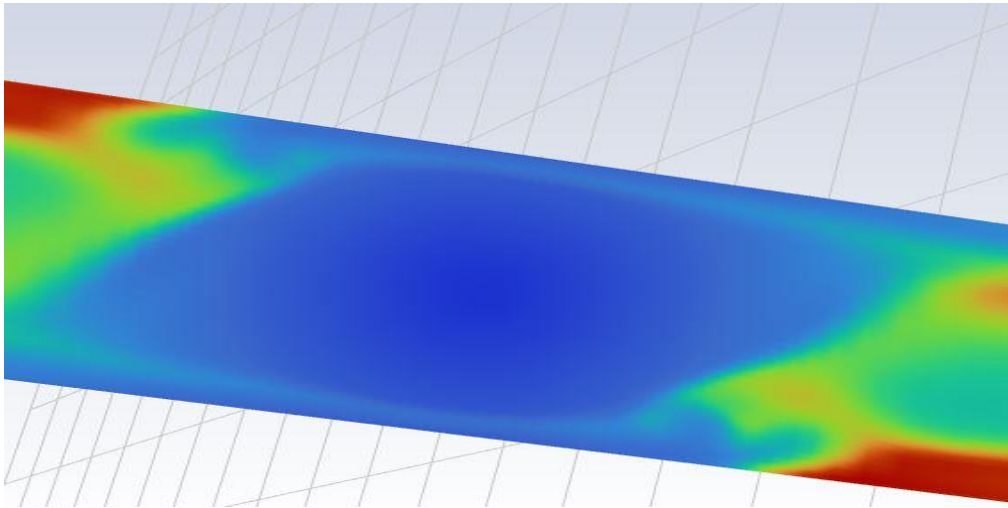


Fig.7.7 Variation Temperature distribution on target plate surface.

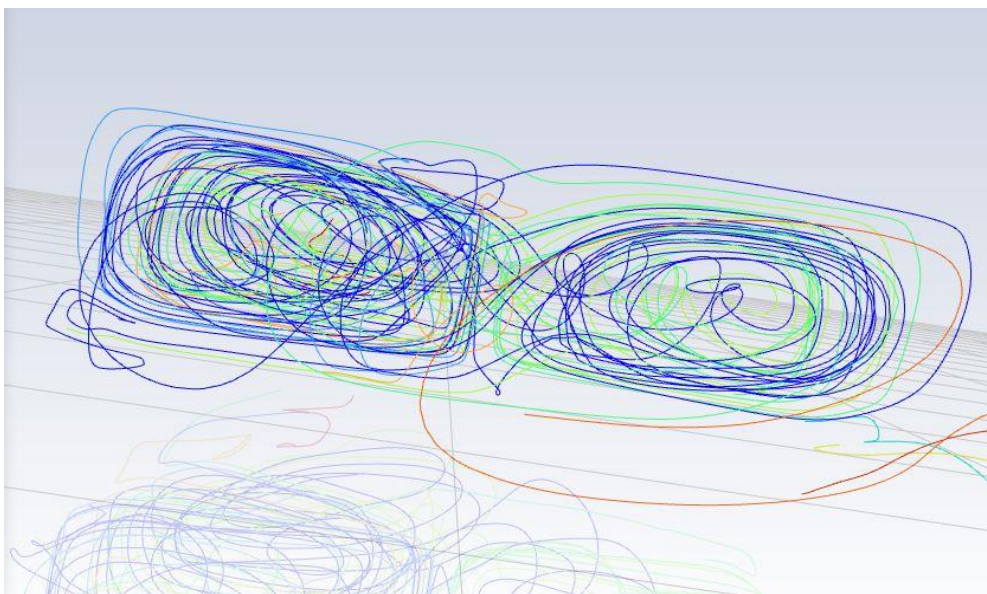


Fig. 7.8 Pathlines of air jet impingement.

In summary, the static temperature distribution on the hot plate plays an important role in determining the heat transfer performance of synthetic jet cooling. A uniform temperature distribution on the hot plate is preferred for optimal cooling performance. Numerical simulations can be used to study the effect of the static temperature distribution on the hot plate and to optimize the cooling performance.

### 7.9 EFFECT OF STATIC VELOCITY DISTRIBUTION

The static velocity distribution in the vicinity of the hot surface also has a significant effect on the heat transfer performance of synthetic jet cooling. The static velocity distribution affects the convective heat transfer coefficient by influencing the flow field and the transport of heat away from the hot surface. Fig. 7.9 and 7.10 shows the velocity distribution and velocity vector of synthetic jet with 2 orifices. The velocity is maximum at the inlet and minimum near the hot plate surface. Numerical analysis can help optimize the jet nozzle geometry and operating conditions to achieve the desired velocity distribution and cooling performance. The simulations can also provide insight into the underlying physical mechanisms that govern the heat transfer process in synthetic jet cooling.

Higher static velocity on the hot surface leads to a higher heat transfer rate due to the increased fluid mixing and convective transport of heat away from the hot surface. However, the velocity distribution should be uniform to avoid flow instabilities or stagnation regions that reduce the heat transfer coefficient.

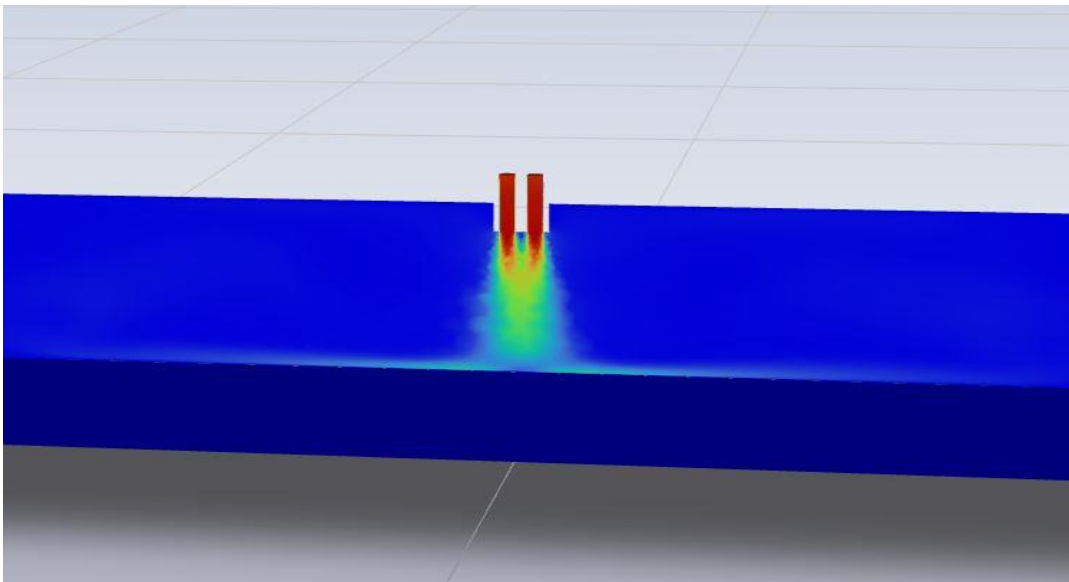


Fig. 7.9 Velocity distribution in 2 orifices.

In summary, the static velocity distribution on the hot surface plays a critical role in determining the heat transfer performance of synthetic jet cooling. Uniform velocity distribution is preferred for optimal cooling performance, and numerical simulations can be used to optimize the jet nozzle geometry and operating conditions for the desired velocity distribution and cooling performance.

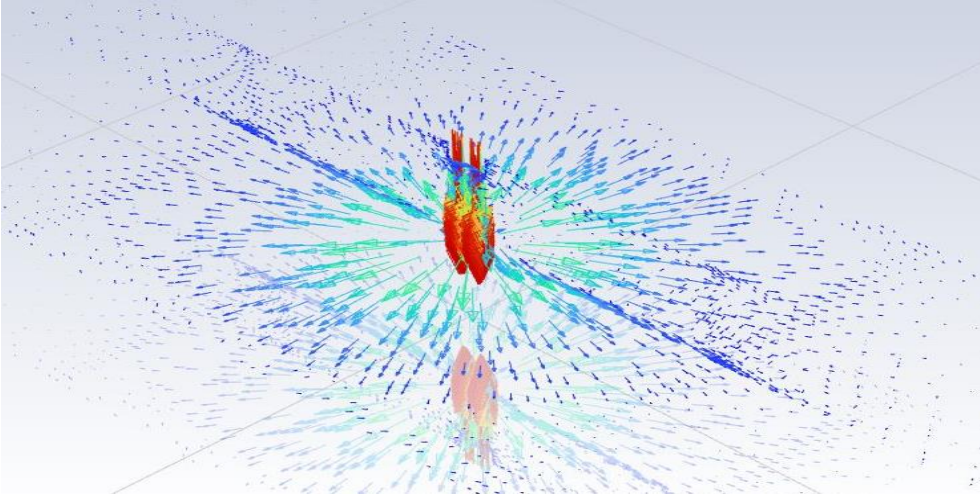


Fig.7.10 Velocity vector.

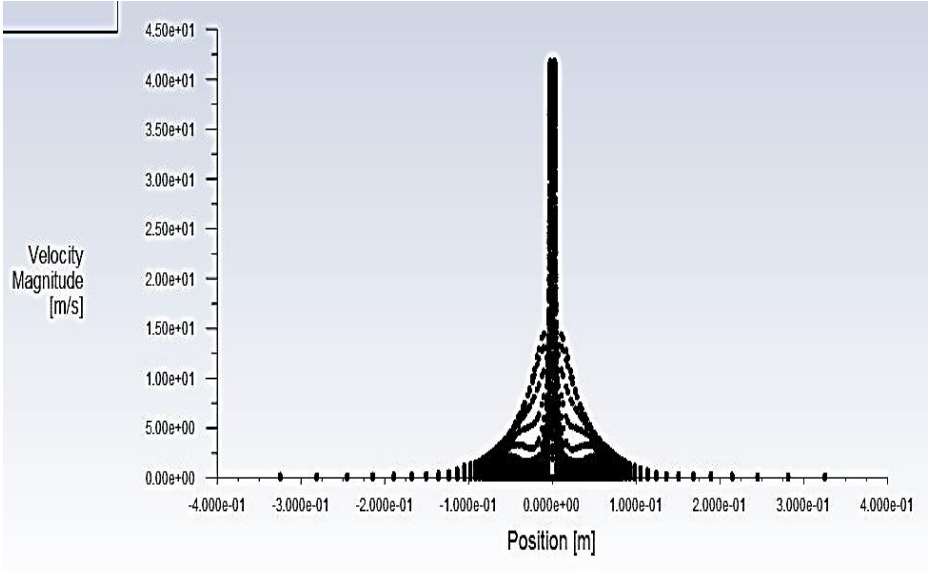


Fig.7.11 Variation of Velocity in radial direction of the plate for 2orifices.

The variation of velocity in the radial direction of the plate for 2 orifices in synthetic jet impingement cooling depends on the operating conditions of the synthetic jet, the geometry of the jet nozzle, and the distance between the nozzle and the hot plate.

The velocity in the radial direction will decrease as the distance from the nozzle increases. This is because the velocity of the synthetic jet decreases as it travels away from the nozzle due to frictional losses and entrainment of the surrounding fluid. In a two-orifice synthetic jet impingement cooling system, the velocity distribution in the radial direction can be affected by the distance between the orifices and the orientation of the jets. The interaction between the two jets can lead to complex flow patterns and vortices that affect the velocity distribution in the radial direction. Fig.7.11 shows the variation of velocity in radial direction of the plate for 2orifices.

In summary, the variation of velocity in the radial direction for a two-orifice synthetic jet impingement cooling system depends on the operating conditions, jet nozzle geometry, and distance between the nozzle and the hot plate.

## CHAPTER 6: CONCLUSION AND SCOPE OF FUTURE WORK

### 6.1 CONCLUSIONS

A numerical investigation was carried out to study the effects of frequency, Reynolds number, and Strouhal number on the heat transfer characteristics of synthetic jet cooling. The analysis is done with multiple orifice (2,4 and 16 orifices) with different operating frequencies ( $f=100\text{Hz}$  to  $f=500\text{Hz}$  and  $f=1\text{Hz}$  to  $f=5\text{Hz}$ ) with different Reynolds numbers ( $Re=5000$ ,  $10000$  and  $20000$ ) well as Strouhal number ( $St=0.006$  to  $St=0.030$ ). The results indicate that as the frequency increases, the average Nusselt number increases for all plates with increase in number orifices. Multiple orifice exhibits higher heat transfer rate as compared to the single orifice with same diameter. A correlation is proposed for average Nusselt number in terms of Reynolds number which is valid for air as the cooling medium. The variation trend of  $Nu_A$  with flow time largely depends on  $St$  and its magnitude depends on  $Re$ . At constant frequency, the average Nusselt number goes up as decrease in Strouhal number. Smaller  $St$  can only be generated by larger  $Re$ . Variation in the value of Strouhal number affects the heat removal capacity of synthetic jet. At a constant Reynolds number, the stroke length decreases with frequency. As  $St$  improves, turbulence kinetic energy rises, resulting in more violent mixing and a better cooling effect. A correlation is proposed for average Nusselt number in terms of Strouhal number for a constant frequency. There is a limit to the number of orifices that can be used to cool a certain region or area effectively. The behaviour of the jets changes as the number of orifices increases, to become a continuous jet. Overall, synthetic jet impingement cooling is a promising technique for high heat flux cooling applications, and the optimization of its performance requires careful consideration of the various parameters that affect the heat transfer performance.

## 6.2 SCOPE OF FUTURE WORK

Considering the present level of comprehension and findings from this study, the following recommendations are put forward for future research:

- (a) Other excitation methods can be employed to compare the results obtained in this study, such as the use of acoustic actuators.
- (b) The impact of the angle at which the jet strikes the surface can also be investigated by altering the jet impingement angle with the surface plate.
- (c) To examine the same flow rates, it is suggested that a comparative study of jets and droplets be carried out, varying droplet parameters such as droplet spacing, frequency, and jet impingement parameters such as nozzle diameter.
- (d) To explore the impact of turbulence on heat transfer performance, studies focusing on turbulent flows in jets and droplets at higher Reynolds numbers after impingement should be conducted.
- (e) While the present study assumed no phase change due to lower heat flux assumptions, upcoming studies may explore the effects of higher heat flux heat transfer rates by incorporating phase change mechanisms like boiling/evaporation.
- (f) In order to better simulate practical scenarios, research on heat surface boundary conditions other than constant heat flux should be conducted.
- (g) The performance of Synthetic jet for cooling electronic devices is analysed by examining Synthetic jet actuators based heat sinks and microchannels. Compared to conventional fan-based heat sinks, lower thermal resistance is reported for Synthetic jet based heat sinks. However, fewer studies have been conducted on micro Synthetic jet actuators based heat sinks and microchannels for miniature electronic devices using both active and passive cooling techniques.

## REFERENCES

1. Arun Jacob, K.A. Shafi, K.E.Reby Roy(2021), “Heat transfer characteristics of piston-driven synthetic jet”, *International Journal of Thermofluids*, 11 100104.
2. Carlo Salvatore Greco, Gennaro Cardone, Julio Soria(2017), “On the behaviour of impinging zero-net-mass-flux jets”, *Journal of Fluid Mechanics*,vol.810,pp.25-59. Cambridge University Press 2016, doi:10.1017/jfm.2016.703.
3. F.F. Cadec(1968), “Fundamental Investigation of Jet Impingement Heat Transfer” , Ph.D Thesis, University of Cincinnati, USA.
4. Laxmikant Mangate, Harekrishna Yadav, Amit Agrawal, Mangesh Chaudhari(2019), “Experimental investigation on thermal and flow characteristics of synthetic jet with multiple-orifice of different shapes”. *International Journal of Thermal Sciences* 140 344–357.
5. M. Chaudhari, B. Puranik, A. Agrawal(2010), “Heat Transfer Analysis in a Rectangular Duct Without and With Cross-Flow and an Impinging Synthetic Jet, *IEEE TRANSACTIONS ON COMPONENTS AND PACKAGING TECHNOLOGIES*”, Volume 33, Issue 2 488-497.
6. M. Chaudhari, B. Puranik, A. Agrawal(2011), “Multiple orifice synthetic jet for improvement in impingement heat transfer”, *International Journal of Heat and Mass Transfer* 54 2056-2065.
7. M. Jain, B. Puranik, A. Agrawal(2011), “A numerical investigation of effects of cavity and orifice parameters on the characteristics of a synthetic jet flow”, *Sens. Actuators, A* 165 351–366.
8. Museong Kim , Hoonsang Lee , Wontae Hwang(2021), “Experimental study on the flow interaction between two synthetic jets emanating from a dual round orifice”, *Experimental Thermal and Fluid Science* 126 110400.
9. O. Manca , P. Mesolella , S. Nardini , D. Ricci(2011) , “Numerical study of a confined slot impinging jet with nanofluids”, *Nanoscale Res. Lett.*6 (1)188 .
10. Pavlova, M. Amitay(2006), “Electronic Cooling Using Synthetic Jet Impingement”, *Journal of Heat Transfer*, 128 897-907.
11. Ping Li, Dingzhang Guo, Ruirui Liu(2019), “Mechanism analysis of heat transfer and flow structure of periodic pulsating nanofluids slot-jet impingement with different waveforms”, *Applied Thermal Engineering* 152 937–945.

12. Ping Li, Xinyue Huang, Dingzhang Guo(2020), “Numerical analysis of dominant parameters in synthetic impinging jet heat transfer process”, *International Journal of Heat and Mass Transfer* 150 119280.
13. Robert Gardon, J. Cahit Akfirat(1966), “Heat transfer characteristics of two dimensional air jets”, *ASME J. Heat Transf.* 88 (1) 101–107 .
14. R. Mahalingam(2007), “Modeling of Synthetic Jet Ejectors for Electronics Cooling”, *23rd Annual IEEE Semiconductor Thermal Measurement and Management Symposium* 196-199.
15. R. Mahalingam, N. Rumigny, A. Glezer(2004), “Thermal Management Using Synthetic Jet Ejectors”, *IEEE TRANSACTIONS ON COMPONENTS AND PACKAGING TECHNOLOGIES*, Volume 27, Issue 3 439-444.
16. R. Mahalingam, A. Glezer(2005), “Design and Thermal Characteristics of a Synthetic Jet Ejector Heat Sink”, *Journal of Electronic Packaging, Transactions of the ASME* 127 172-177.
17. Zhuo Liu, Qinghua Yu, Ziyue Mei, and Danmei Xie(2019), “Impingement Cooling Performance Analysis and Improvement of Synthetic Jets for Electronic Devices”, *Journal Of Thermophysics And Heat Transfer* Vol. 33, , pp. 856-864.

